Contrib Mineral Petrol (2007) 153:251–271
DOI 10.1007/s00410-006-0145-9

ORIGINAL PAPER

Relationships between O isotope equilibrium, mineral alteration and Rb–Sr chronometric validity in granitoids: implications for determination of cooling rate

Jiang Feng Chen · Yong-Fei Zheng · Zi-Fu Zhao · Bo Li · Zhi Xie · Bing Gong · Hui Qian

Received: 10 May 2006 / Accepted: 14 September 2006 / Published online: 13 October 2006
© Springer-Verlag 2006

Abstract A combined study of mineral O and Rb–Sr isotopes was carried out for a number of Mesozoic granitoids in China in order to compare the degree of O isotope equilibrium between coexisting minerals, with the validity of mineral Rb–Sr isochrons for granitoids. A scrutiny of both O isotope geothermometry and Rb–Sr internal isochron dating for corresponding minerals indicates that equilibrium O isotope fractionation between Rb–Sr isochron minerals corresponds to geologically meaningful isochron ages if the variation in $^{87}Rb/^{86}Sr$ ratio is big enough to provide reasonably small uncertainties in age. Significant deviation of the Rb–Sr isochron age from the actual age appears to depend on the difference in Sr isotopic composition between an external fluid and the igneous minerals. As a result, O isotope disequilibrium is often caused by interaction between the rock and the external fluid that results in mineral alteration. Post-magmatic alteration can cause isotope exchange between the minerals and an internally buffered fluid that is isotopically identical to the host rock. The O isotope composition of coexisting minerals in studied samples changed principally due to a decrease in temperature. Both Rb and Sr concentrations and the Sr isotope ratios of isochron minerals also changed due to the mixing of different Sr reservoirs. Nevertheless, the isochron age can remain unchanged if the mixing took place along the isochron chord between the internal fluid and the minerals from that newly altered minerals formed. This provides an insight into the effect of internal and external fluids on the validity of mineral Rb–Sr chronometry. In addition, an alternative approach is proposed to construct the cooling curve by a combined use of O isotope temperature and mineral isotope age for the granitoids of interest. Comparing with the traditional method using the empirical closure temperature for Rb–Sr chronometry, the proposed approach utilizes fewer variables with smaller uncertainties than the traditional way.

Keywords Minerals · Rb–Sr isochron · O isotope temperature · Equilibrium state · Diffusion · Fluid · Granite

Communicated by: J. Hoefs.

J. F. Chen · Y.-F. Zheng (✉) · Z.-F. Zhao · B. Li · Z. Xie · B. Gong · H. Qian
CAS Key Laboratory of Crust-Mantle Materials and Environments, School of Earth and Space Sciences, University of Science and Technology of China, Hefei 230026, China
e-mail: yfzheng@ustc.edu.cn

Introduction

Whole-rock and mineral Rb–Sr dating has long been a routine practice of granitoid geochronology (e.g., Faure 1986; Dickin 1995) despite the increasing applications of zircon U–Pb dating. A geologically meaningful isochron age for a suite of cogenetic samples can be obtained only when all analyzed samples were formed at the same time, possessed the same initial Sr isotopic ratio, and only if the system remained closed throughout its geological history (e.g., Faure and Powell 1977; Zheng 1989). The MSWD (mean squared weighted deviation) of an isochron is a widely accepted parameter to judge if these prerequisites were justified The MSWD value tells whether the uncertainty in the calculated isochron ages is caused by the analytical

methods only, but not by any geological facts, such as heterogeneity in the initial Sr isotopic ratios (e.g., Brooks et al. 1972; Wendt and Carl 1991; Ludwig 1999). However, this statistical method is only an internal test. Sometimes, geologically spurious ages are obtained because of isotopic disequilibrium between isochron minerals, or disturbance of previously attained equilibrium (e.g., Juteau et al. 1984). Therefore, the state of equilibrium and disequilibrium has to be recognized comprehensively not only by means of chromomeric systems, but also by other isotopic systems (e.g., O), as well as geochemical and petrological characteristics (Zheng et al. 2002, 2003a).

Recent studies have demonstrated that the state of O isotope equilibrium between metamorphic minerals can provide a test for the validity of mineral Sm–Nd and Rb–Sr chronometers. Zheng et al. (2002) observed a direct correspondence in the state of equilibrium or disequilibrium between the O and Sm–Nd isotopic systems of minerals in ultrahigh pressure eclogites from the Sulu orogen in East-Central China. Some omphacite–garnet pairs from the eclogites yielded O isotope equilibrium fractionations at eclogite-facies conditions and the minerals gave meaningful Triassic Sm–Nd isochron ages. In contrast, other omphacite–garnet pairs yielded O isotope disequilibrium fractionations and mineral Sm–Nd isochrons yielded meaningless non-Triassic ages. Similar conclusions were reached for eclogite and gneiss at Shuanghe in the Dabie orogen (Zheng et al. 2003a), for a garnet peridotite at Zhimafang in the Sulu orogen (Zheng et al. 2003b) and for eclogites in the Dabie orogen (Li et al. 2003; Xie et al. 2004). The question, therefore is, can the same methodology be applied for granites?

A critical premise in evaluating the validity of either mineral isochron or O isotope geothermometry is, whether the isotopic systems in question have achieved thermodynamic equilibrium at the time of their formation, or later isotopic re-equilibration due to a late geological event. If these two conditions were not met, the isochron does not date a geological event, and the $\delta^{18}O$ difference between coexisting minerals cannot be used for geothermometry. If the thermodynamic equilibrium has been achieved and preserved, then not only does the isochron give a meaningful age of a given geological event (original crystallization or metamorphism), but the $\delta^{18}O$ differences between minerals also provide temperatures for O isotope equilibrium at the time of rock formation. Diffusion plays a key role in the distribution of trace elements and isotopes within and among minerals in igneous rocks (e.g., Giletti 1986; Eiler et al. 1993; Zheng et al. 2003a). Equilibrium and disequilibrium among minerals are principally controlled by the diffusion of elements and isotopes in coexisting minerals, if dissolution–recrystallization is not significant during a given geological process (Zheng et al. 1999a, 2004a).

In the temperature range at which most granitic rocks crystallize and cool, that is at about 800–300°C, the general order of diffusivity is as follows (Fig. 1): Sr, O and Ar in hornblende diffuse the slowest, then Sr in oligoclase and biotite and O in quartz, O in feldspars and biotite and Ar in biotite diffuse the fastest. Closure temperatures can be calculated using diffusion coefficient and the equation of Dodson (1973). Assuming an effective diffusion radius (a half of grain size) of 1 mm and a cooling rate of 10°C/Ma, the closure temperature of Sr diffusion is about 680°C in hornblende, 415°C in biotite and 620°C in oligoclase (Giletti 1991; Giletti and Casserly 1994; Brabander and Giletti 1995); that of O diffusion is about 565°C in hornblende, 350°C in biotite, 380°C in quartz and 225–255°C in feldspars (Giletti et al. 1978; Giletti and Yund 1984; Farver and Giletti 1985; Fortier and Giletti 1991); that of Ar diffusion is about 610°C in hornblende and 380°C in biotite (Harrison 1981; Harrison et al. 1985). However, the closure temperatures depend on effective diffusion radii, cooling rates of the systems involved and diffusion coefficients of the elements in the minerals (Dodson 1973, 1979), which are further affected by chemical composition and grain size of the minerals (Harrison et al. 1985; Hodges 2003). Numerically, uncertainty in either activation energy (Q) or pre-exponential factor (Do) could cause an uncertainty in closure temperature up to 100°C.

Taking into account the large uncertainties in estimated cooling rate and effective diffusion radius, the

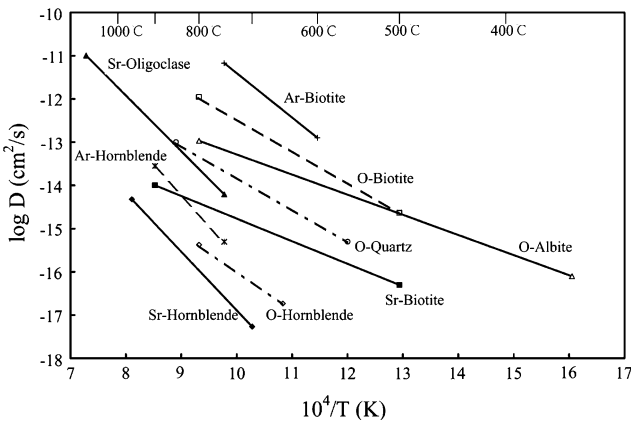

Fig. 1 Plot of diffusion coefficients of Sr, O and Ar in hornblende, biotite, plagioclase and quartz vs. temperature. Data after Giletti et al. (1978), Harrison (1981), Giletti and Yund (1984), Farver and Giletti (1985), Harrison et al. (1985), Fortier and Giletti (1991), Giletti (1991), Giletti and Casserly (1994) and Brabander and Giletti (1995)

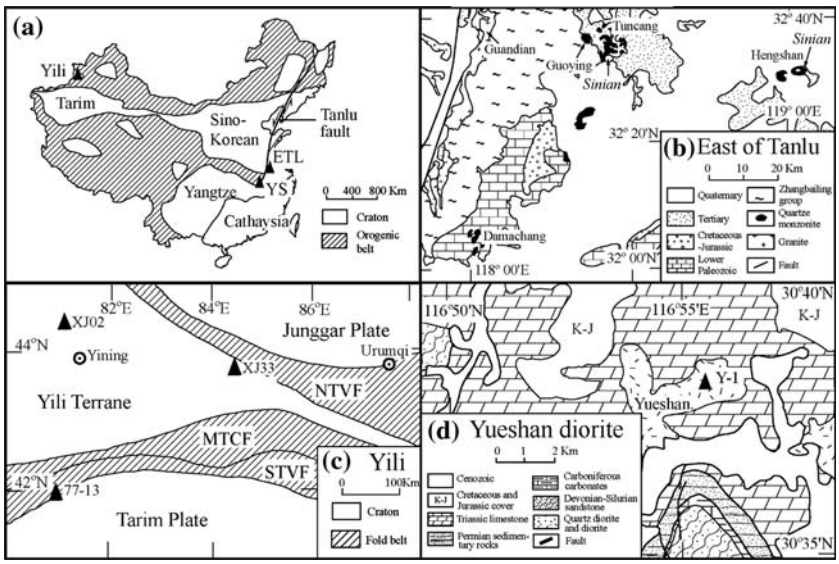

Fig. 2 Geologic sketches of the studied regions. *Solid triangles* denote the sample regions and locations. **a** Location map of the studied regions (modified after Zhang et al. 1984); *ETL*, *Yili* and *YS* stand for the region east of the Tanlu fault, the Yili terrane and the Yueshan intrusion. **b** The region east of the Tanlu fault (modified after map of Anhui 1987, b). **c** A sketch of tectonic division of Yili and adjacent regions (modified after Xiao et al. 1990; Xinjiang 1993). *XJ02*, *77-13* and *XJ33* represent the sample locations for these samples. *NTVF*, *MTCF* and *STVF* represent the North Tianshan Late Paleozoic (Variscan) fold belt, the Middle Tianshan Early Paleozoic (Caledonian) fold belt and the South Tianshan Late Paleozoic (Variscan) fold belt. **d** The Yueshan quartz diorite (modified after Anhui 1970a, b)

uncertainty in closure temperature could be even larger. If the same size of rock specimen is investigated nevertheless, the cooling rate and effective diffusion radius remain the same and thus uncertainties in the cooling rate and effective diffusion radius basically cancel each other out. The above estimates are based on the assumption of diffusion exchange with an infinite reservoir (Dodson 1973, 1979). The mode of the rock and diffusion mechanism could also be taken into account (Giletti 1986; Eiler et al. 1993; Jenkin et al. 1991, 1994, 1995; Jenkin 1997; Zhao et al. 2004). Worldwide, most granitic rocks show approximately the same sequence of closure temperatures. The regular sequence of O isotopic temperatures for different quartz–mineral pairs from granitoids has been used to test the idea that diffusion is a dominant factor controlling the closure of both radiometric and O isotopic systems during rock cooling (Zhao et al. 2004).

In a cooling system, if the equilibrium of O isotopes between minerals is achieved, isotopic equilibrium must be achieved for those elements with diffusion coefficients greater than, or similar to those of O diffusion in the same minerals. If the equilibrium of O isotopes is preserved despite later thermal disturbances, isotopic equilibrium for the elements with diffusion coefficients smaller than and similar to those of O diffusion would also be preserved. On the other hand, if the O isotopic equilibrium has not been achieved during cooling, the isotopic equilibrium for the elements with diffusion coefficients smaller than those of O diffusion would not be achieved. If the O isotopic equilibrium has been disturbed because of a later thermal event, the isotopic equilibrium for the elements with diffusion coefficients greater than those of O, would be disturbed. Therefore, an assessment of O isotope equilibrium between minerals, which define a mineral isochron, may provide a means to test the validity of an isochron (Zheng et al. 2002, 2003a).

In practice, however, a series of questions arise. How do O and Rb–Sr isotopes behave during cooling and mineral alteration in granitoids? How does the fluid which might have different origins, and the post-magmatic hydrothermal alteration frequently observed in granitoids, affect O and Rb–Sr isotope systems? Is the internal Rb–Sr isochron age, given by minerals from a hydrothermally altered intrusive rock, geologically meaningless or not? In this paper, we present several case studies to partially answer these questions.

Samples and geological settings

The samples from three localities chosen for this study are four plutons of quartz monzonite that are located east of the Tanlu fault in East-Central China, granites from the Yili terrane in northwest China, and the

Yueshan quartz diorite from the Mid-Lower Yangtze region in East-Central China (Fig. 2).

Quartz monzonites east of the Tanlu fault

The oldest rocks occurring in this region, east of the gigantic sinistral Tanlu fault in East-Central China (Fig. 2a), is the Zhangbaling Group spilite-keratophyre sequence of middle Neoproterozoic age that experienced blueschist to greenschist facies metamorphism during the Triassic continental collision between the Yangtze Block and the North China Block (Cong 1996; Zheng et al. 2003c, 2005). Overlying the middle Neoproterozoic rocks are the typical Yangtze-type sedimentary cover that consists of Upper Neoproterozoic to Paleozoic clastic and carbonate sedimentary rocks. Mesozoic terrestrial clastic sedimentary and volcanic rocks are distributed in the basins (Anhui 1987, b; Fig. 2b). A group of intrusions consisting of quartz monzonite in composition with early Cretaceous ages crop out in the region. Four intrusive bodies (Hengshan, Tuncang, Guoying and Damachang) were chosen for this study (Fig. 2b). Among them the Damachang body is associated with gold deposit (Anhui 1987, b). The four intrusions are similar mineralogically, but differ in texture, mode and the nature of their country rock. Hornblende, biotite, plagioclase and quartz were separated from the four quartz monzonites.

The Tuncang body intrudes into the schist of the Zhangbaling group as well as dolomite and limestone of Upper Neoproterozoic (Fig. 2b). The rock shows porphyritic texture with phenocrysts of plagioclase, potassium feldspar (K-feldspar), and minor quartz and hornblende. The K-feldspar phenocryst is microperthite, and often contains plagioclase, quartz, hornblende, biotite and titanite as ingredient materials. The largest K-feldspar phenocryst measures as long as 5 cm. The plagioclase phenocryst shows albite twin and vague zoning with An of 22–29. The grandmass contains plagioclase (An = 0–29), K-feldspar, quartz, hornblende, biotite and minor opaque minerals with a grain size of about 3 mm. The studied sample 96D71 was collected from a quarry and is fresh with only very weak chloritization of biotite, but common in argillation of K-feldspar.

The Hengshan body intrudes into the dolomite of Upper Neoproterozoic and is covered by Neogene basalt at its central part (Fig. 2b). The rock shows subhedral heterogranular texture with a grain size of about 1–3 mm for most of the constituent minerals. The rock consists of plagioclase (~36% with An = 15–29), K-feldspar (~33%), quartz (~21%), hornblende (~5%), biotite (~3%) and minor opaque minerals. The studied sample 96D61 was collected from a quarry and is fresh with weak chloritization of biotite and argillation of K-feldspar.

The Guoying body intrudes into the schist of the Zhangbaling group and is unconformably covered by the Neogene basalt at its eastern part (Fig. 2b). The rock shows subhedral heterogranular texture with a grain size of about 1–3 mm. The rock consists of plagioclase (~39% with An = 10–29), K-feldspar (~12%), quartz (~20%), hornblende (~10%), biotite (~10%) and minor opaque minerals. The studied sample 96D81 shows weak chloritization of biotite and hornblende and weak sericitization of plagioclase.

The Damachang body intrudes into the dolomite and limestone of the Lower Paleozoic (Fig. 2b). The rock shows subhedral heterogranular texture with a grain size of about 1–3 mm for most of the constitute minerals. The rock consists of plagioclase (~31% with An = 15–29), K-feldspar (~30%), quartz (~23%), hornblende (~7%), biotite (~8%) and minor opaque minerals. The studied sample 96D93 was collected from an exploratory drift of a gold mine, but away from the ore body. The sample is fresh with weak chloritization of biotite, but commonly displays argillation of K-feldspar.

Granites from the Yili terrane in northwest China

The Yili terrane, located in Xinjiang, Northwest China, is a part of the Kazakstein-Yili microplate, within the giant Central-Asia Orogenic belt (Sengor et al. 1993; Fig. 2a). The terrane is bordered to the Tarim plate at the south by Mid-Tianshan Early Paleozoic fold belt and South-Tianshan Late Paleozoic fold belt and to the Junggar microplate at the north by North-Tianshan Late Paleozoic fold belt (Xiao et al. 1990; Fig. 2c). The Yili terrane possesses a Proterozoic basement and is covered by Paleozoic and Mesozoic sedimentary and volcanic rocks. Many granitic intrusions crop out along the periphery of the terrane (Xinjiang 1993). Three granites are chosen for this study.

The Yingmanlai alkaline feldspar granite in the South-Tianshan Late Paleozoic fold belt (Fig. 2c) intruded into Precambrian gneiss. The studied sample 77-13 is coarse grained (grain size of 5–6 mm) and consists of microcline, plagioclase, biotite and minor muscovite. Fluorite is occasionally observed. Biotite is fresh, while feldspars are highly altered.

The Ertai hornblende monzogranite is located near the northern margin of the Yili terrane (Fig. 2c) and intruded into Silurian and Devonian clastic rocks. It is assigned as Late Paleozoic in age based on the field observation (Xinjiang 1993). The sample studied (XJ02) shows the granitic texture with a grain size of 2–

5 mm and contains perthite, plagioclase, quartz, biotite, hornblende and minor apatite. Myrmekite can be observed under microscope. The hornblende is fresh; however, the biotite shows chrolitization, K-feldspar argillation and plagioclase sericitization.

The sample XJ33 was collected from the east of the Yili terrane (Fig. 2c). The rock body intruded into Carboniferous pyroclastic rocks and was overlaid by Jurassic clastic rocks. The sample is granite with a grain size of 2–5 mm, composed of perthite, plagioclase, quartz and biotite. Myrmekite can be seen under microscope. The rock specimen is highly weathered. Biotite shows chloritization and feldspars sericitization, while hornblende is relatively fresh. Based on the field observation, the rock body is Late Paleozoic in age (Xinjiang 1993).

Quartz diorite at Yueshan in the Middle-Lower Yangtze region, east-central China

The Yueshan diorite crops out in the northern margin of the Yangtze Block in east-central China (Fig. 2a). The rock intruded into Permian and Triassic dolomite, limestone, gypsiferous horizon and clastic sedimentary rocks (Fig. 2d). Hornfels, marble and skarn were formed along the contacts. The intrusive body consists of diorite, quartz diorite and locally oligosite. Quartz diorite occurs near the contact with sandstone where quartz increases in the rock and albite molecules increase in the plagioclase because of assimilation of high silica and alumina material.

The studied sample Y-1 is a quartz diorite, collected from at a depth of about 420 m from a drill hole, located in the eastern part of the intrusive body (Fig. 2d). The sample is fresh and free from weathering. The rock shows subhedral texture with grain size of 0.03–2.5 mm. The sample contains plagioclase (~60%, including oligoclase and andesite with An = 14–35 and albite), K-feldspar (~8%), quartz (~8%), hornblende (~16%), biotite (~3%) and accessory minerals (2%, aptite, titanite, magnetite and zircon). The andesite shows zoning. K-feldspar is mostly orthoclase, with minor microcline and cryptoperthite, which replaced and, thus, were later than the plagioclase and quartz. Biotite was partially replaced by chlorite and plagioclase by kaolinite.

Hornblende, biotite, plagioclase and quartz were separated from the sample Y-1. Biotite was further separated into two aliquots, one was fresh, free from alteration and the other was altered. The plagioclase was further separated into three parts, the fresh one, the weakly altered one and the altered one, according to their diaphaneity. Hornblende was not further separated, because it was free from alteration. K-feldspars from all the studied rocks were not separated and analyzed because of common alteration.

Analytical methods

Rock samples were crushed to 80 mesh size and minerals were separated gravitationally and magnetically, followed by hand picking under a binocular microscope. During separation, the small grains and rim of the mineral grains were preferentially removed so that the results most probably represent only the isotope compositions of mineral grains bigger than 80 mesh size.

O isotopes

Oxygen isotope analyses were carried out at the Laboratory for Chemical Geodynamics, University of Science and Technology of China (USTC), by the laser fluorination technique (Sharp 1990) with a 25-W MIR-10 CO_2 laser (Zheng et al. 2002). The O_2 produced was directly transferred to the Delta+ mass spectrometer for the measurements of $^{18}O/^{16}O$ ratios (Rumble et al. 1997). The three reference minerals used were: $\delta^{18}O = 5.8‰$ for garnet UWG-2 (Valley et al. 1995), $\delta^{18}O = 5.2‰$ for olivine SCO-1 (Eiler et al. 1995) and $\delta^{18}O = 10.0‰$ for zircon 91500 (Zheng et al. 2004b). In order to test the analytical quality of quartz and feldspar, furthermore, three different quartz standards were used: $\delta^{18}O = 11.1‰$ for the National Standard of China GBW04409, $\delta^{18}O = -1.7‰$ for the National Standard of China GBW04410, and $\delta^{18}O = 9.6‰$ for the International Standard NBS-28. Reproducibility for repeated measurements of each sample is given in Table 1. About half of the samples give reproducibility for $\delta^{18}O$ better than ± 0.1‰, but about another half better than ± 0.2‰, with a few slightly worth than that. Assuming preservation of O isotopic equilibration at the scale of sample measurement, apparent equilibrium temperatures were calculated using on the calibration of Zheng (1993a, b) with uncertainties in 2σ. Judgment and interpretation of O isotope equilibrium or disequilibrium between coexisting minerals are based on measured fractionation values and resultant sequence of O isotope temperatures in combination with rates of O diffusion in concerned minerals and corresponding sequence of closure temperatures (Giletti 1986; Zheng and Fu 1998; Zhao et al. 2004).

Rb–Sr isotopes

Analyses of Rb and Sr concentrations and Sr isotopic compositions were carried out at the Laboratory for

Table 1 Oxygen isotopic ratios for the single minerals from Mesozoic granitoids in China

Sample number	Mineral	$\delta^{18}O$ (‰)	Pair	$\Delta^{18}O_{Q-X}$ (‰)	T (°C)[a]	$\pm\Delta T$ (°C)[b]
Quartz monzonites east of the Tanlu fault						
Tuncang						
96D71Q	Quartz	8.89, 8.80				
96D71P	Plagioclase	6.57, 6.57	Qtz–Pl[c]	2.28	385	40
96D71H	Hornblende	4.97, 4.86	Qtz–Hbl	3.93	545	25
96D71B	Biotite	3.94, 3.78	Qtz–Bt	4.99	460	20
Damachang						
96D93Q	Quartz	9.68, 9.43				
96D93P	Plagioclase	6.38, 6.43	Qtz–Pl[c]	3.15	255	25
96D93H	Hornblende	5.67, 5.50	Qtz–Hbl	3.97	540	25
96D93B	Biotite	3.29, 3.41	Qtz–Bt	6.21	360	15
Hengshan						
96D61Q	Quartz	9.45, 9.50				
96D61P	Plagioclase	6.49, 6.67	Qtz–Pl[c]	2.90	285	30
96D61H	Hornblende	5.36, 5.45	Qtz–Hbl	4.07	530	25
96D61B	Biotite	3.63, 3.72	Qtz–Bt	5.80	390	15
Guoying						
96D81	Quartz	8.48, 8.56				
96D81F	Plagioclase	5.36, 5.40	Qtz–Pl[c]	3.14	255	25
96D81H	Hornblende	4.82, 5.02	Qtz–Hbl	3.60	590	30
96D81B	Biotite	3.15, 2.91	Qtz–Bt	5.49	415	15
Granites in the Yili plate						
Yingmanlai granite						
77-13Q	Quartz	10.28, 10.44				
77-13F	Plagioclase	10.08, 10.21	Qtz–Pl[c]	0.21	>1,600	
77-13B	Biotite	7.16, 7.04	Qtz–Bt	3.26	675	35
Ertai granite						
XJ02Q	Quartz	9.67, 9.73				
XJ02Pl	Plagioclase	7.86, 8.01	Qtz–Pl[c]	1.76	505	60
XJ02B	Biotite	1.32, 1.46	Qtz–Bt	8.31	250	10
Granite in eastern Yili						
XJ33Q	Quartz	11.91, 12.11				
XJ33F	Plagioclase	8.99, 9.18	Qtz–Pl[c]	2.92	285	30
XJ33B	Biotite	2.32, 2.26	Qtz–Bt	9.72	200	5
Quartz diorite at Yueshan						
Y-1Q	Quartz	10.27, 10.43				
Y-1P	Plagioclase	7.21, 7.35	Qtz–Pl[d]	3.07	295	30
Y-1Pwa	Plagioclase (weakly altered)	7.13, 7.34	Qtz–Plwa	3.11	290	30
Y-1Pa	Plagioclase (altered)	7.70, 7.78	Qtz–Pla[d]	2.61	360	35
Y-1H	Hornblende	5.73, 5.81	Qtz–Hbl	4.58	470	20
Y-1B	Biotite	3.71, 3.92	Qtz–Bt	6.53	340	15
Y-1Ba	Biotite (altered)	3.26, 3.33	Qtz–Bta	7.05	310	10

[a] Oxygen isotope temperatures were calculated based on the theoretical calibration of Zheng (1993a, b)

[b] Uncertainty in O isotope temperature is quoted based on the average reproducibility of ± 0.15‰ for $\delta^{18}O$ values and the error propagation from fractionation equations

[c] Calculated assuming An = 20 for plagioclase

[d] Calculated assuming An = 30 for plagioclase

Chemical Geodynamics, USTC, using the procedure modified after Foland and Allen (1991). Samples were dissolved in the mixed acid (HF + HNO_3) in the sealed Savillex beakers on hot plate. Separation of Rb and Sr was performed via a routine ion exchange technique using Bio-Rad 50 × 8 cation resin. The Rb and Sr concentrations were analyzed by isotope dilution. Rb and Sr isotopic ratios were measured on a Finnigan MAT-262 mass spectrometer with seven movable collectors. Sr isotopic ratios were normalized to $^{86}Sr/^{88}Sr = 0.119400$. The procedural blank is below 1 ng for Rb and 2 ng for Sr. During the period of data

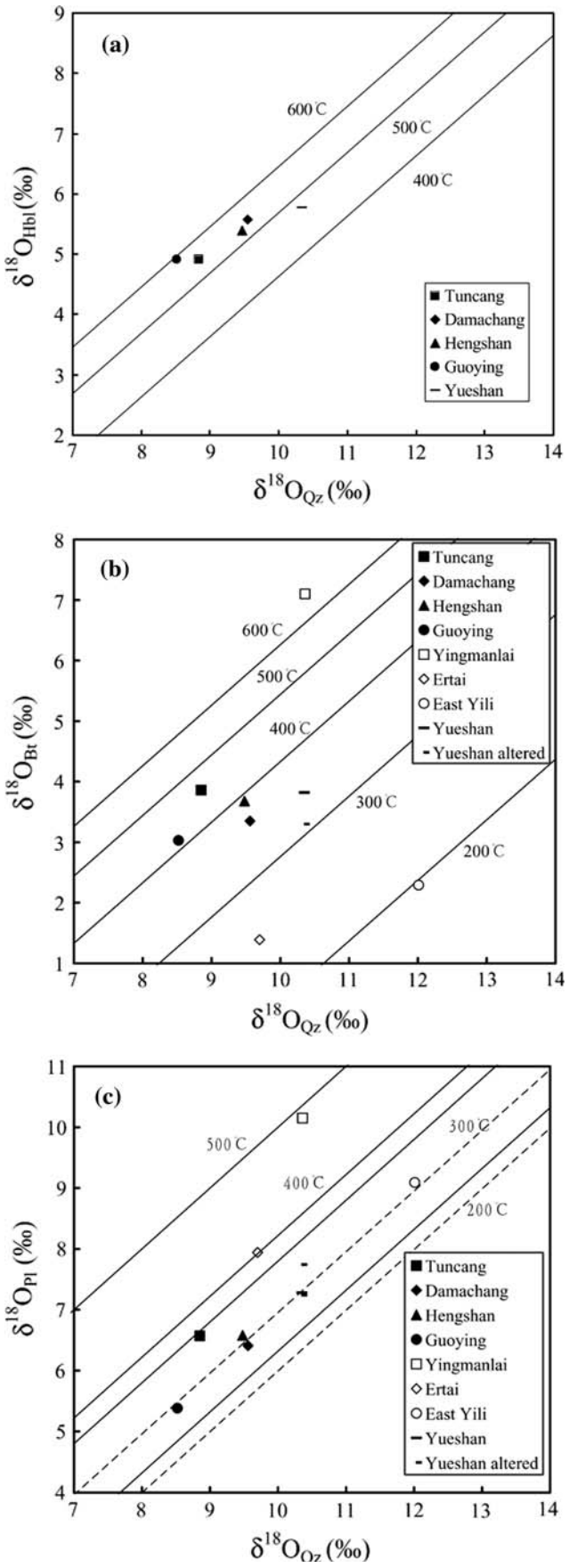

◀ **Fig. 3** $\delta^{18}O_{Qz}$ vs. $\delta^{18}O_{Hbl}$ (**a**), $\delta^{18}O_{Bt}$ (**b**) and $\delta^{18}O_{Pl}$ (**c**) plots for granitoids east of the Tanlu fault, Yili terrane and the Yueshan quartz diorite, respectively. Isotherms are calculated after the theoretical calibration of Zheng (1993a, b). *Solid and dashed lines* in **c** denote the plagioclase with An = 20 and 30, respectively

acquisition, the interlaboratory reference material SRM987 gave the value $^{87}Sr/^{86}Sr = 0.710253 \pm 0.000032$ ($n = 38$) and BCR-1 gave Rb of 47.04 ± 0.10 ppm, Sr of 330.7 ± 2.0 ppm and $^{87}Sr/^{88}Sr = 0.705006 \pm 0.000027$, which agree with the compilation given by Gladney et al. (1990), within uncertainties. Precision in the determined $^{87}Rb/^{86}Sr$ and $^{87}Sr/^{86}Sr$ of 1 and 0.01% is assigned, respectively, based on the analyses of reference materials. Rb–Sr isochron ages were calculated using program ISOPLOT (Ludwig 1999).

Results

O isotope temperatures

Quartz monzonites east of the Tanlu fault

As listed in Table 1, all the four quartz monzonites show the same sequence of ^{18}O enrichment in the minerals as follows: quartz > plagioclase > hornblende > biotite. The Tuncang quartz monzonite gives quartz–hornblende temperature (T_{Q-Hbl}) of 545 ± 25°C, quartz–biotite temperature (T_{Q-Bt}) of 460 ± 20°C and quartz–plagioclase temperature (T_{Q-Pl}) of 385 ± 40°C, respectively. The Damachang intrusion yields T_{Q-Hbl} of 540 ± 25°C, T_{Q-Bt} of 360 ± 15°C and T_{Q-Pl} of 255 ± 25°C, respectively. The Hengshan body gives T_{Q-Hbl}, T_{Q-Bt} and T_{Q-Pl} of 530 ± 25, 390 ± 15 and 285 ± 30°C, respectively. The Guoying body yields T_{Q-Hbl}, T_{Q-Bt} and T_{Q-Pl} of 590 ± 30, 415 ± 15 and 255 ± 25°C, respectively.

Hornblende has the slowest rate of O diffusion relative to the other minerals (Zheng and Fu 1998). When paired with quartz, it gives high temperatures of 530 ± 25 to 590 ± 30°C for all the four intrusions. This suggests preservation of high-T O isotope equilibria between hornblende and quartz. All the four intrusions show that the T_{Q-Hbl} is higher than the T_{Q-Bt} and the T_{Q-Bt} is higher than the T_{Q-Pl} (Fig. 3). It appears that the minerals with faster diffusivity give lower O isotope temperatures. The sequence of the observed O isotope temperatures indicates that retrograde isotopic re-equilibration or exchange with matrix minerals might have continuously occurred during cooling of the intrusions in a closed system (Giletti 1986; Zhao et al. 2004).

Granites from the Yili terrane

The quartz samples of the three granites show high $\delta^{18}O$ values ranging from 9.70 to 12.01‰ (Table 1), consistent with the range of S-type granites (O'Neil and Chappell 1977). However, magnitude and sequence of quartz–mineral $\delta^{18}O$ differences are not consistent with equilibrium fractionations at any reasonable temperature. Sample 77-13 from the Yingmanlai granite shows very similar $\delta^{18}O_Q$ and $\delta^{18}O_{Pl}$ values to each other, yielding unreasonably high T_{Q-Pl} of > 1,600°C and T_{Q-Bt} of 675 ± 35°C (Table 1; Fig. 3).

Sample XJ02 shows $\delta^{18}O_Q > \delta^{18}O_{Pl} > \delta^{18}O_{Bt}$, but gives a reversed sequence of O isotope temperatures in which T_{Q-Pl} of 505 ± 60°C is higher than T_{Q-Bt} of 250 ± 10°C (Table 1; Fig. 3). This relation is inconsistent with the known sequence of equilibrium temperature in which T_{Q-Bt} is higher than T_{Q-Pl} as predicted by the closure temperature of O diffusion in biotite and plagioclase (Zheng and Fu 1998). Sample XJ33 has mineral O isotopic relations that are very similar to sample XJ02. It shows $\delta^{18}O_Q > \delta^{18}O_{Pl} > \delta^{18}O_{Bt}$, but T_{Q-Pl} of 285 ± 30°C is higher than the T_{Q-Pl} of 200 ± 5°C (Table 1; Fig. 3).

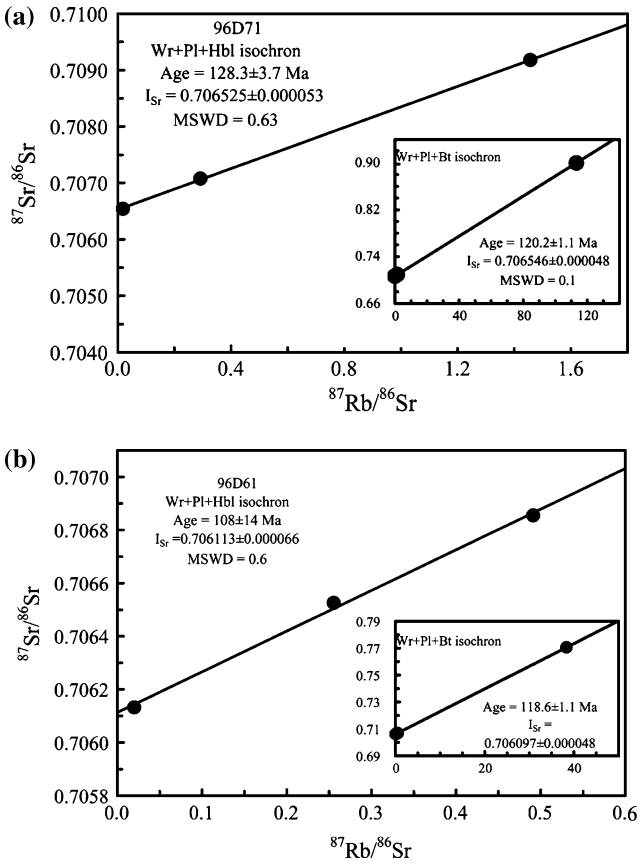

Fig. 4 Rb–Sr isochrons for the Tuncang and Hengshan quartz monzonites from the east of the Tanlu fault. **a** Wr + Hbl + Pl isochron of the Tuncang body and the *inset* shows its Wr + Pl + Bt isochron, **b** Wr + Hbl + Pl isochron of the Hengshan body and the *inset* shows its Wr + Pl + Bt isochron

Quartz diorite at Yueshan

The unaltered minerals from the Y-1 show that $\delta^{18}O_Q > \delta^{18}O_{Pl} > \delta^{18}O_{Hbl} > \delta^{18}O_{Bt}$ (Table 1). The sample gives O isotope temperatures of 470 ± 20°C for T_{Q-Hbl}, 340 ± 15°C for T_{Q-Bt} and 295 ± 30°C for T_{Q-Pl}, respectively (Table 1; Fig. 3). The O isotopic relation between the unaltered minerals suggests retrograde re-equilibration during the cooling of the rock. However, an altered biotite–quartz pair gives an O isotope temperature of 310 ± 10°C, which is marginally lower than T_{Q-Bt} of 340 ± 15°C; an altered plagioclase–quartz pair yields a temperature of 360 ± 35°C, which is also marginally higher than that of T_{Q-Pl} of 295 ± 30°C. These suggest that the $\delta^{18}O$ differences involving the altered biotite and plagioclase might have been shifted slightly from the equilibrium fractionation values due to post-magmatic alteration.

Rb–Sr isochrons

Quartz monzonites east of the Tanlu fault

The whole-rock + hornblende + plagioclase (Wr + Hbl + Pl, as short) Rb–Sr isochron of the Tuncang body gives an age of 128.3 ± 3.7 Ma and an initial $^{87}Sr/^{86}Sr$ ratio of 0.706525 ± 0.000053 with MSWD = 0.6 (Table 3; Fig. 4a). On a $^{87}Rb/^{86}Sr$ vs. $^{87}Sr/^{86}Sr$ plot, whole-rock + hornblende + plagioclase + biotite (Wr + Hbl + Pl + Bt, as short) yields a linear arrangement giving an ''isochron'' age of 120.2 ± 2.5 Ma with a large MSWD value of 8.4 suggesting a somewhat poor linearity. This is caused by the fact that only the biotite plots off the regression line due to isotopic exchange either with the other minerals during cooling in a closed system (e.g., Jenkin et al. 1995; Jenkin 1997) or with externally derived fluid, thus resulting in a heterogeneity in Sr isotopic ratios for the isochron minerals at the time when the biotite became closed to Sr diffusion. However, both Sr concentration and Sr isotopic ratio of feldspar will change very little since Sr in the rock is dominant by feldspars. In this case, plagioclase + biotite (Pl + Bi) isochron carries clear geological meaning, recording the time when Sr in biotite was closed to diffusion. Since the slope of the isochron is controlled by the biotite with high Rb/Sr ratio, the whole-rock + plagioclase + biotite (Wr + Pl + Bt) and Pl + Bi isochrons give the same age and initial ratios despite the

uncertainty in the initial ratios are slightly larger for Pl + Bi isochron. Wr + Pl + Bt isochron of the Tuncang body gives an age of 120.2 ± 1.1 Ma and an initial $^{87}Sr/^{86}Sr$ ratio of 0.706546 ± 0.000048, identical to the age and initial ratio given by Wr + Hbl + Pl + Bt isochron, but with much smaller uncertainties and MSWD = 2.0 (Table 3 and inset of Fig. 4a).

Similar to the Tuncang body, the Damachang body yields a Wr + Hbl + Pl Rb–Sr isochron age of 131 ± 6 Ma and an initial Sr ratio of 0.706038 ± 0.000060 with a MSWD = 0.1 (Table 3). Its Wr + Pl + Bt Rb–Sr isochron gives an age of 120.2 ± 1.1 Ma and an initial $^{87}Sr/^{86}Sr$ ratio of 0.706073 ± 0.000047 with MSWD = 1.1 (Table 3).

On the Rb–Sr isochron plot, the Hengshan body yields a Wr + Hbl + Pl linear arrangement corresponding to an age of 108 ± 14 Ma and an initial $^{87}Sr/^{86}Sr$ ratio of 0.706113 ± 0.000066 with MSWD = 0.6 (Table 3; Fig. 4b). Its Wr + Pl + Bt Rb–Sr isochron gives an age of 118.6 ± 1.1 Ma and an initial $^{87}Sr/^{86}Sr$ ratio of 0.706097 ± 0.000048 with MSWD = 0.003 (Table 3 and inset of Fig. 4b).

The Guoying body is very similar to the Hengshan. The Wr + Hbl + Pl linear arrangement yields a poorly constrained Rb–Sr isochron age of 128 ± 29 Ma and an initial $^{87}Sr/^{86}Sr$ ratio of 0.70762 ± 0.00013 with MSWD = 0.5 (Table 3). The Wr + Pl + Bt Rb–Sr isochron gives an age of 126.7 ± 1.2 Ma and an initial $^{87}Sr/^{86}Sr$ ratio of 0.707635 ± 0.000047 with MSWD = 0.3 (Table 3).

In the above cases, the Sr initial isotopic ratios given by Wr + Hbl + Pl and Wr + Pl + Bt isochrons are the same for the individual intrusions. This suggests that the Sr isotopic ratios in the rock systems were controlled by plagioclase that has the highest Sr concentration but the lowest Sr isotopic ratio in the isochron minerals.

Granites from the Yili terrane

The Wr + Pl + Bt isochron of the Yingmanlai granite (77-13) gives a poorly constrained age of 167 ± 15 Ma and an initial $^{87}Sr/^{86}Sr$ of 0.764 ± 0.093 with MSWD = 849 (Table 3; Fig. 5a). The ''isochron'' age matches a K–Ar age of 159 Ma (Tuomeur 1985). Sample XJ02 from the Ertai granite yields a Wr + Pl + Bt Rb–Sr ''isochron'' age of 203 ± 50 Ma and an initial $^{87}Sr/^{86}Sr$ of 0.7117 ± 0.0027 with MSWD = 70 (Table 3; Fig. 5b). Sample XJ33 gives a Wr + Pl + Bt Rb–Sr ''isochron'' age of 241 ± 15 Ma and an initial $^{87}Sr/^{86}Sr$ of 0.7081 ± 0.0026 with a large MSWD value of 146 (Table 3; Fig. 5c). All the three granites from the Yili terrane share very large MSWD values and very large uncertainties in both initial ratio and isochron age. This may be caused by the presence of Sr isotope heterogeneity in the isochron minerals, which could have existed at the time the biotite became closed to Sr diffusion.

Quartz diorite at Yueshan

The isochron constructed by three unaltered minerals (Hbl, Bt and Pl) from the Yueshan quartz diorite yields an age of 137.6 ± 1.3 Ma and an initial $^{87}Sr/^{86}Sr$ of 0.706319 ± 0.000047 with MSWD = 0.3 (Table 3; Fig. 6). A total of six minerals, including unaltered and altered ones, form an isochron giving an age of 136.86 ± 0.85 Ma and an initial $^{87}Sr/^{86}Sr$ of 0.706320 ± 0.000034 with MSWD = 1.0 (Table 3; Fig. 6). The Rb and Sr concentrations and the Sr isotopic ratios of the altered biotite and plagioclase were changed relative to those of the unaltered minerals because of alteration. The altered biotite gives lower $^{87}Rb/^{86}Sr$ and $^{87}Sr/^{86}Sr$ ratios of 17.93 and 0.741052 ± 0.000016, respectively, than those of 57.68 and 0.819140 ± 0.00002 for the unaltered biotite (Table 2). In contrast, the altered plagioclase gives higher $^{87}Rb/^{86}Sr$ and $^{87}Sr/^{86}Sr$ ratios of 0.120 and 0.706523 ± 0.000016, respectively, than those of 0.029 and 0.706389 ± 0.000017 for the unaltered one (Table 2). Although the Rb and Sr concentrations and the Sr isotopic ratios were changed by alteration, the isochron constructed by the unaltered minerals only overlaps the isochron constructed by both altered and unaltered minerals, showing excellent collinearity (Fig. 6).

Correspondence in the state of O isotope equilibrium with the validity of Rb–Sr isochron

So far, only limited geochronological work has been carried out for intrusions from the regions east of the Tanlu fault. Li et al. (1985) reported a zircon U–Pb age of 128 ± 1 Ma for the Guandian monzogranite, an intrusion just west of the studied region (Fig. 2b). Chen et al. (2003) dated the Tuncang and Hengshan quartz monzonites by the $^{40}Ar/^{39}Ar$ technique and gave plateau ages of 125.51 ± 0.55 and 125.7 ± 1.8 Ma for hornblendes, and 118.0 ± 0.1 and 120.0 ± 0.2 Ma for biotite for the two bodies, respectively.

For the Tuncang quartz monzonite, the Wr + Hbl + Pl Rb–Sr isochron age of 128.3 ± 3.7 Ma obtained from this study (Table 3; Fig. 4a) agrees with a hornblende Ar–Ar plateau age of 125.51 ± 0.55 Ma (Chen et al. 2003) within the analytical uncertainties. Hence, the Wr + Hbl + Pl Rb–Sr isochron age is geo-

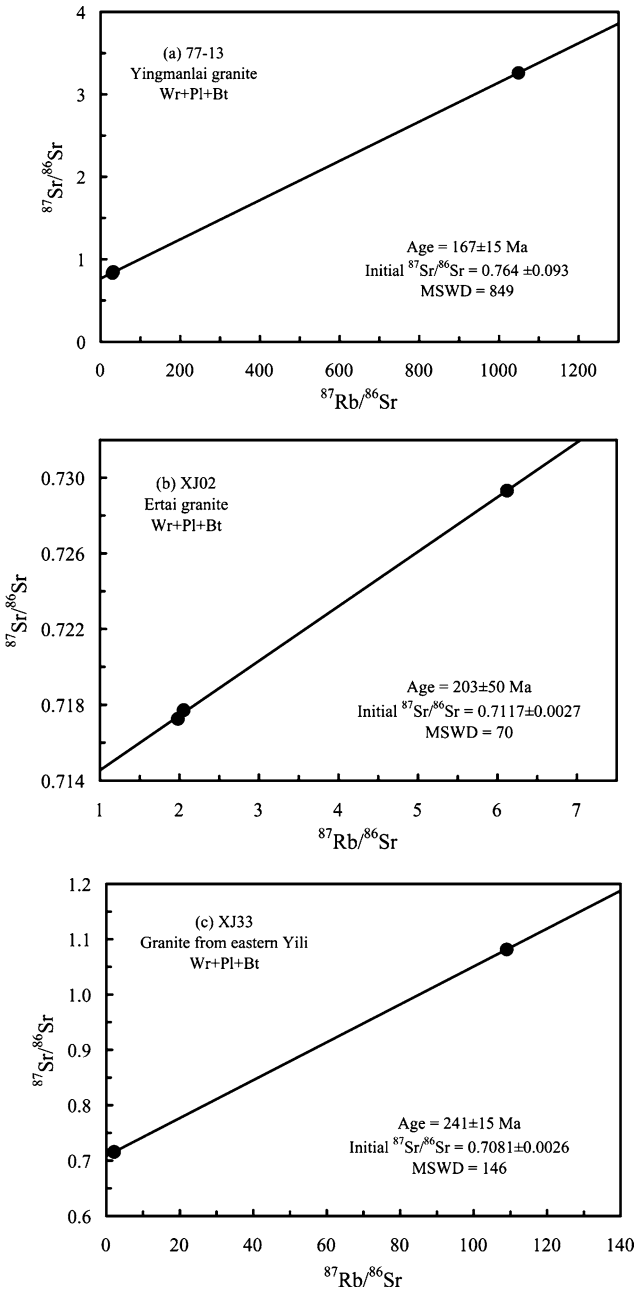

Fig. 5 Wr + Pl + Bt Rb–Sr isochrones for the granites from the Yili terrane: **a** the Yingmanlai granite, **b** the Ertai granite, **c** the granite from the eastern Yili

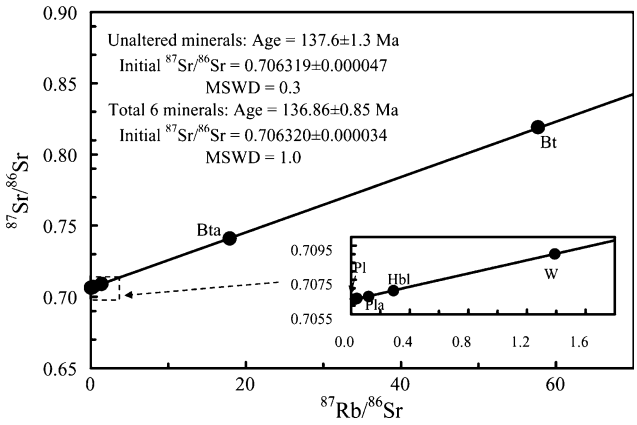

Fig. 6 Rb–Sr isochrons for the Yueshan quartz diorite in Mid-Lower Yangtze region. The isochron constructed by three unaltered minerals gives an age of 137.6 ± 1.3 Ma and an initial $^{87}Sr/^{86}Sr$ = 0.706319 ± 0.000047 with a MSWD = 0.3, that by unaltered and altered (total six) minerals gives an age of 136.86 ± 0.85 Ma and an initial $^{87}Sr/^{86}Sr$ = 0.706320 ± 0.000034 with a MSWD = 1.0. The isochron formed by calculated ''whole-rock'' together with unaltered and altered minerals gives an age of 136.85 ± 0.79 Ma and an initial $^{87}Sr/^{86}Sr$ = 0.706308 ± 0.000077 with a MSWD = 1.0. The three isochrones are indistinguishable

logically meaningful. The good collinearity and the small MSWD value for the Wr + Hbl + Pl Rb–Sr isochron suggest that the hornblende and plagioclase have the same initial Sr isotopic ratios, and that the time interval of Sr diffusion closure from hornblende to plagioclase is not distinguishable by the present chronometer, if the closure temperatures predicted by the Dodson (1973) equation alone are reasonable. This implies that the Sr isotopic ratios of plagioclase would not change by diffusion exchange of Sr isotopes between hornblende and plagioclase because of the much higher Sr content of plagioclase. The Wr + Hbl + Pl Rb–Sr isochron age is thus interpreted as the time when the rock was cooled to the Sr closure temperatures in the hornblende (at ~680°C). The Ar–Ar plateau age is interpreted as the time when the rock was cooled to the closure temperature of Ar diffusion in hornblende (at ~610°C). The agreement, within the uncertainties, between those apparent ages implies fast cooling, after solidification of the intrusion (above ~700°C). The rapid cooling in the high-T stage is frequently observed in many intrusions (e.g., Chen et al. 1995; Zheng et al. 1996; Zhao et al. 2004).

Meanwhile, the normal sequence of O isotopic temperatures ($T_{Q-H} > T_{Q-B} > T_{Q-Pl}$) suggests that the rock-forming minerals crystallized under equilibrium conditions and then continuously re-equilibrated by diffusion exchange during cooling. Re-equilibration of O isotopes took place at temperatures below ~460°C (T_{Q-Bt}). Since the confirmation of diffusion mechanism in a rock system is a precondition for the reasonable application of closure temperature concept to chronometric systems (Zhao et al. 2004), the comparability between the Sr diffusion closure temperature and the O isotopic temperature suggests that the state of O isotope equilibrium corresponds to a geologically meaningful Rb–Sr isochron.

The Wr + Pl + Bt isochron for the Tuncang body shows a good collinearity. The Wr + Pl + Bt isochron

Table 2 Rb and Sr concentrations and Sr isotopic ratios for Mesozoic granitoids in China

Sample number	Mineral	Rb (ppm)	Sr (ppm)	$^{87}Rb/^{86}Sr$	$^{87}Sr/^{86}Sr$	±[a]
Quartz monzonites east of the Tanlu fault						
Tuncang						
96D71	Whole rock	85.98	852.6	0.292	0.707077	17
96D71F	Plagioclase	10.03	1,621	0.018	0.706540	15
96D71H	Hornblende	18.80	37.34	1.457	0.709179	21
96D71B	Biotite	423.6	11.03	113.2	0.899927	21
Damachang						
96D93	Whole rock	123.4	911.3	0.392	0.706764	18
96D93F	Plagioclase	32.36	1,771	0.053	0.706137	18
96D93H	Hornblende	19.67	54.38	1.047	0.707983	16
96D93B	Biotite	506.3	18.94	78.35	0.839872	18
Hengshan						
96D61	Whole rock	77.88	882.1	0.255	0.706526	13
96D61F	Plagioclase	12.28	1,785	0.020	0.706132	16
96D61H	Hornblende	9.04	53.24	0.491	0.706855	16
96D61B	Biotite	245.5	18.66	38.31	0.770664	19
Guoying						
96D81	Whole rock	94.42	839.0	0.326	0.708237	18
96D81F	Plagioclase	66.58	1,132	0.170	0.707927	14
96D81H	Hornblende	9.37	70.00	0.387	0.708316	16
96D81B	Biotite	540.4	14.75	108.0	0.902133	22
Country rocks						
96D77	Proterozoic schist	19.60	75.70	0.750	0.713263	16
96D95	Paleozoic shale	93.20	1,859	0.145	0.709899	18
Granites in the Yili terrane						
Yingmanlai granite						
77-13	Whole rock	314.7	30.63	30.07	0.828372	20
77-13F	Plagioclase	413.0	38.17	31.93	0.846980	22
77-13B	Biotite	1,887	6.506	1,049	3.261030	49
Ertai granite						
XJ02	Whole rock	154.5	225.8	1.981	0.717253	17
XJ02F	Plagioclase	249.1	351.4	2.053	0.717715	17
XJ02B	Biotite	81.37	39.11	6.121	0.729320	17
Granite in eastern Yili						
XJ33	Whole rock	140.6	189.4	2.149	0.715252	16
XJ33F	Plagioclase	179.7	243.5	2.137	0.715603	16
XJ33B	Biotite	480.4	13.22	109.0	1.081470	24
Quartz diorite at Yueshan						
Y-1P	Plagioclase	27.94	2,821	0.029	0.706389	17
Y-1Pwa	Plagioclase (weakly altered)	34.20	2,502	0.040	0.706427	18
Y-1Pa	Plagioclase (altered)	83.43	2,020	0.120	0.706523	16
Y-1H	Hornblende	5.680	56.76	0.289	0.706872	14
Y-1B	Biotite	500.4	25.38	57.68	0.819140	20
Y-1Ba	Biotite (altered)	315.0	51.00	17.93	0.741052	16

[a] Uncertainties in determined $^{87}Sr/^{86}Sr$ represented by the last two digits

age of 120.2 ± 1.1 Ma (Table 3 and inset of Fig. 4a) is close to a biotite Ar–Ar age of 118.0 ± 0.1 Ma (Chen et al. 2003). Therefore, the Wr + Pl + Bt Rb–Sr isochron age is also geologically meaningful, and thus, interpreted as the time when the rock was cooled to the closure temperature of Sr diffusion in biotite (~415°C). The biotite Ar–Ar age is interpreted as the time when the rock was cooled to the closure temperatures of Ar diffusion in biotite (~380°C).

Based on the Dodson (1973) concept for closure temperature alone (e.g., Giletti and Casserly 1994), after Sr diffusion was closed in hornblende and plagioclase, Sr could continuously exchange between biotite and such mineral(s) with low Sr closure temperature(s) as apatite. However, because the intrusion in question is young and mass balance shows a predominance of Sr budget in biotite relative to apatite, the Sr isotopic ratio of biotite would change very little.

Table 3 Rb–Sr isochron ages for Mesozoic granitoids in China

Pluton name	Sample number	Mineral and rock assemblage[a]	$(^{87}Rb/^{86}Sr)_{max}$	Ages (Ma)	$(^{87}Sr/^{86}Sr)_i$	±[b]	MSWD
Quartz monzonites east of the Tanlu fault							
Tuncang	96D71	Wr + Pl + Hbl	1.5	128.3 ± 3.7	0.706525	53	0.6
		Wr + Pl + Bt	113	120.2 ± 1.1	0.706546	48	2.0
Damachang	96D93	Wr + Pl + Hbl	1.0	131 ± 6	0.706038	60	0.1
		Wr + Pl + Bt	78	120.2 ± 1.1	0.706073	47	1.1
Hengshan	96D61	Wr + Pl + Hbl	0.5	108 ± 14	0.706113	66	0.6
		Wr + Pl + Bt	38	118.6 ± 1.1	0.706097	48	0.003
Guoying	96D81	Wr + Pl + Hbl	0.4	128 ± 29	0.70762	13	0.5
		Wr + Pl + Bt	108	126.7 ± 1.2	0.707635	47	0.3
Granites in the Yili terrane							
Yingmanlai	77-13	Wr + Pl + Bt	1,050	167 ± 15	0.764	93	849
Ertai	XJ02	Wr + Pl + Bt	6.1	203 ± 50	0.7117	27	70
East Yili	XJ33	Wr + Pl + Bt	109	241 ± 15	0.7081	26	146
Quartz diorite at Yueshan							
Yueshan	Y-1	Pl + Hbl + Bt	58	137.6 ± 1.3	0.706319	47	0.3
		Pl + Hbl + Bt + Pl_{wa} + Pl_a + Bt_a	58	136.86 ± 0.85	0.706320	34	1.0

[a] *Wr*, *Pl*, *Hbl* and *Bt* stand for whole-rock, plagioclase, hornblende and biotite, respectively. Subscripts wa and a denote the weakly altered and altered, respectively

[b] Uncertainties in determined $^{87}Sr/^{86}Sr$ represented by the last two digits

The young Rb–Sr isochron age is likely caused by exchange of Sr isotopes between biotite and an externally derived fluid during cooling. In fact, the country rocks of these intrusions possess much lower $^{87}Sr/^{86}Sr$ ratios than the biotite at $t = 120$ Ma (Table 2). The difference between the Wr + Hbl + Pl and Wr + Pl + Bt isochron ages is larger than the uncertainties, suggesting a slow cooling from ~680 to ~415°C.

The Damachang body is similar to the Tuncang quartz monzonite in terms of the relationship between the Rb–Sr isochron age and the O isotope temperature. The Wr + Hbl + Pl Rb–Sr isochron age of 131 ± 6 Ma is indistinguishable from a zircon U–Pb age of 128 ± 1 Ma for the Guandian body (Li et al. 1985) and a hornblende Ar–Ar age of 125.51 ± 0.55 Ma for the Tuncang body (Chen et al. 2003). Therefore, the Damachang Wr + Hbl + Pl Rb–Sr isochron age is geologically meaningful, representing the time of the Sr diffusion closure in hornblende. The Wr + Pl + Bt Rb–Sr isochron age of 120.2 ± 1.1 Ma is identical to the Wr + Pl + Bt Rb–Sr isochron age and close to the biotite Ar–Ar ages for the Tuncang body, and thus is also geologically meaningful and represents the time when the Sr was closed in biotite. The geologically meaningful Rb–Sr isochron ages again correspond to the retrograde re-equilibration of O isotope exchange between the minerals ($T_{Q-Hbl} > T_{Q-Bt} > T_{Q-Pl}$; Table 1).

Sample 96D61 from the Hengshan body is similar to the Tuncang intrusion in that they show retrograde O isotope re-equilibration between the minerals with the relation of $T_{Q-Hbl} > T_{Q-Bt} > T_{Q-Pl}$. Unlike the Tuncang body, however, the Wr + Hbl + Pl Rb–Sr ''isochron'' age of 108 ± 14 Ma for the Hengshan intrusion not only carries the large uncertainty, but also is younger than the hornblende Ar–Ar age of 125.7 ± 1.8 Ma, and thus its precise geological meaning is obscured. Two possible reasons could explain the observation. First, the range in $^{87}Rb/^{86}Sr$ ratios is too small (smaller than 0.5; Tables 2, 3; Fig. 4b), but precision of the isochron age is inversely proportional to the variation range of $^{87}Rb/^{86}Sr$ ratios. Second, assuming a reasonable precision for the determined $^{87}Sr/^{86}Sr$ ratios of 0.01 or 0.02%, at such a small $^{87}Rb/^{86}Sr$ range, the precision of the isochron age would be ± 10 or ± 20 Ma. Obviously, the precise Rb–Sr isochron age can only be obtained when the variation range of $^{87}Rb/^{86}Sr$ is large enough. In addition, the purity of the analyzed minerals should be taken into account. We checked the plagioclase concentrate of the sample under microscope and found that about 5% K-feldspar is mixed with the plagioclase separate, with kaolinitization for some of the K-feldspar. Hence both Sr concentration and $^{87}Sr/^{86}Sr$ ratio of the plagioclase and whole-rock points changed due to the alteration, resulting in the deviation of the isochron age from the true age as represented by the hornblende Ar–Ar age. The country rock shows much higher $^{87}Sr/^{86}Sr$ ratios than quartz monzonites at the age of intrusion (Table 2). The fluid, resulting in alteration of K-feldspar in the Hengshan sample was probably derived from the country rock with elevated $^{87}Sr/^{86}Sr$ ratios. The alteration increased the $^{87}Sr/^{86}Sr$ ratio of the K-feldspar and the ''plagioclase'' mineral separates that contain small amount of K-feldspar impurity, leading to a decrease in the apparent Rb–Sr isochron age. Because the Wr + Pl + Bt Rb–Sr isochron for the Hengshan body is

essentially a 2-point one and the slope of the isochron is thus controlled by biotite with the high $^{87}Rb/^{86}Sr$ ratio (Table 2 and inset of Fig. 4b). A small, age uncertainty is generally associated with this kind of 2-points isochron. The Wr + Pl + Bt Rb–Sr isochron age for the Hengshan body is slightly younger than the biotite Ar–Ar age for the same intrusion. This may also be caused by the impurity (altered K-feldspar) in the plagioclase concentrate and the increase in $^{87}Sr/^{86}Sr$ ratio for the plagioclase.

The Guoying body is similar to the Hengshan quartz monzonite. Sample 96D81 from the body shows retrograde O isotope re-equilibration between the minerals, with the sequence of O isotope temperatures at $T_{Q-Hbl} > T_{Q-Bt} > T_{Q-Pl}$. However, the Wr + Hbl + Pl Rb–Sr ''isochron'' age of 128 ± 29 Ma for the intrusion carries a very large uncertainty and cannot be used to date geological event. Similar to the Hengshan body, the variation range of $^{87}Rb/^{86}Sr$ is very small (smaller than 0.4; Tables 2, 3) for the Guoying sample 96D81, resulting in a large uncertainty in the ''isochron'' age. The Wr + Pl + Bt Rb–Sr isochron for the Guoying body is also essentially a 2-points one, that is associated with a small age uncertainty, and thus may be geologically meaningful (Table 3).

In contrast to the intrusions east of the Tanlu fault, the granite samples from the Yili terrane were all collected from road cuts, with moderate weathering on the surface. The Yingmanlai granite (sample 77-13) gives unreasonably high $T_{Q-Pl} > 1{,}600°C$ and T_{Q-Bt} of 675 ± 35°C (Table 1), clearly reflecting a state of O isotope disequilibrium between the minerals. Correspondingly, the Wr + Pl + Bt Rb–Sr isochron yields the age of 167 ± 15 Ma with the large uncertainty of ± 15 Ma and a poor linearity with MSWD value as large as 850 (Table 3; Fig. 5a). However, the apparent Rb–Sr isochron age agrees with the previous biotite Ar–Ar date at 159 Ma. This is because that the slope of the isochron is controlled by biotite with a very high $^{87}Rb/^{86}Sr$ ratio of 1,050 and the biotite is petrographically unaltered.

The same relationship between the O and Rb–Sr isotope systems is also observed in sample XJ02 from the Ertai granite. The state of O isotope disequilibrium between the minerals is suggested by a reversed sequence between T_{Q-Pl} of 505 ± 60°C and T_{Q-Bt} of 250 ± 10°C (Table 1; Fig. 3). Meanwhile, the Wr + Pl + Bt Rb–Sr isochron has the large MSWD value of 70, reflecting a disturbance of Rb–Sr isotopic system, and gives the age of 203 ± 50 Ma with a large age uncertainty (Table 3; Fig. 5b). With such a large uncertainty, no geological meaning can be assigned to the apparent Rb–Sr isochron age.

Sample XJ33 from eastern Yili also shows the reversed sequence of O isotope temperatures between biotite and plagioclase, with T_{Q-Pl} of 285 ± 30°C higher than T_{Q-Bt} of 200 ± 15°C (Table 1). This corresponds to the state of O isotope disequilibrium between the minerals, with the occurrence of mineral alteration, especially for feldspar. The Wr + Pl + Bt Rb–Sr isochron gives the age of 241 ± 15 Ma, with the large MSWD value of 146 (Table 3; Fig. 5c).

The above comparisons show that the state of O isotope equilibrium between the coexisting minerals corresponds to the Rb–Sr mineral isochrons with good linearity as suggested by the small MSWD values and geologically meaningful ages. In contrast, the state of O isotope disequilibrium between the minerals coincides with the poor Rb–Sr mineral isochron, either showing poor collinearities with the large MSWD values, or giving the geologically meaningless ages, or both. This same conclusion was also reached from such combined studies for metamorphic minerals (Zheng et al. 2002, 2003a, b; Li et al. 2003; Xie et al. 2004). The relations of O isotope temperatures shown by the Yili granitoids suggest that processes other than diffusion, would dictate O isotope exchange during cooling to result in the disequilibrium fractionations between the coexisting minerals. The elevated $\delta^{18}O_{Pl}$ value could result from short-lived water–rock interaction at medium to high temperatures (Taylor and Sheppard 1986; Criss et al. 1987; Gregory et al. 1988).

Fluid effects on the state of O isotope equilibrium and the validity of Rb–Sr isochron

It has been a common practice in O isotope studies of igneous and metamorphic rocks to pair quartz and other minerals for the purpose of O isotope geothermometry (e.g., Bottinga and Javoy 1975; Clayton 1981; Giletti 1986; Zheng et al. 1998, 1999b; Valley 2001; Ernst and Rumble 2003; Li et al. 2004; Zhao et al. 2004, 2005; Xie et al. 2004, 2006; Huang et al. 2006; Wu et al. 2006). Potential assumptions behind it are that: (1) SiO_2 would isotopically behave as a pervasively active phase for O diffusion within natural silicate rocks in high-T geological processes (Zheng et al. 2003a), and (2) considerable amounts of deuteric water in the forms of structural hydroxyl and molecular H_2O in nominally anhydrous minerals would not only serve as an effective medium of O isotope exchange between coexisting minerals but also act as an infinite reservoir for retrograde O isotope resetting during rock cooling (Gong et al. 2006). Because differential resetting of mineral $\delta^{18}O$ values can be caused by the difference in

O diffusivity (Zheng and Fu 1998), disequilibrium fractionations between coexisting minerals suggest the effect of hydrothermal alteration in either close or open system (Taylor and Sheppard 1986; Criss et al. 1987; Gregory et al. 1988).

As observed in this study and others, on granitoids, the apparent O isotope temperatures (T_a) are differentially lower than rock-forming temperatures but sequentially correlated with the Dodson closure temperatures (T_c) of O diffusion in the paired minerals. Thus, this correlative sequence is usually explained by diffusion-controlled O isotope exchange during cooling (e.g., Giletti 1986; Zhao et al. 2004; Xie et al. 2006). However, the closure temperature of quartz is typically above that of biotite and feldspar, so it cannot act as an infinite reservoir during cooling of the lower T_c minerals to exchange according to the model of Giletti (1986). Nevertheless, it is noted that the T_c calculations have employed ''wet'' O diffusion coefficients that were measured in the presence of water (e.g., Giletti 1986; Jenkin et al. 1991, 1994; Eiler et al. 1992, 1993; Zhao et al. 2004; Xie et al. 2006; this study). If ''dry'' O diffusion coefficients (measured in the presence of CO_2 or O_2) are employed, calculated T_c are too high to be compatible with the O isotope temperatures of the lower T_c minerals. Thus retrograde O isotope exchange would only occur in the presence of water, to achieve the O isotopic re-equilibration between quartz and the lower T_c minerals. In other words, the diffusion-controlled exchange of O isotopes between coexisting minerals in granitoids would proceed in a H_2O-present system, where the O diffusion is favored by high mobility of molecular H_2O and OH groups (e.g., Zhang et al. 1991; Doremus 2004).

Feldspars have the fastest rate of O diffusion among rock-forming minerals and thus O isotope exchange would cease at the lowest temperatures in granitoids (Giletti 1986). Despite this precept, significant amounts of water from hundreds to thousands of ppm H_2O by weight have been measured in the form of structural hydroxyl and molecular H_2O in nominally anhydrous minerals (e.g., Nakashima et al. 1995; Rossman 1996; Grant et al. 2003; Bell et al. 2004; Johnson and Rossman 2004; Gong et al. 2006). This kind of confined fluidis internally buffered in stable isotope composition and thus, capable of serving as an effective medium of O isotope exchange between quartz and the other minerals. In this regard, it violates the models involving fast grain boundary (FGB) diffusion because water was not taken into account as a phase during cooling. As a result, they yield an unreasonable prediction that suggests strong dependence of O isotope temperatures calculated from mineral-pair fractionations on mineral proportions (Jenkin et al. 1991, 1994; Eiler et al. 1992, 1993). Furthermore, apparent disequilibrium and reversed O isotope fractionation between quartz and feldspar in certain slowly cooling closed-systems was erratically ascribed to the presence of large volume of fast diffusers (biotite and cordierite) or a predominance of magnetite in the system (Jenkin et al. 1991, 1994). Because isotope partitioning between phases is a function of temperature at thermodynamic equilibrium, it is not true that the O isotope fractionations between phases depend on mineral modal abundance.

The problem is that FGB models were constructed on the basis of the assumptions that no water was available for O isotope exchange between coexisting minerals during rock cooling in a closed system and that no uncertainty was associated with the determination of O diffusion coefficients and O isotope fractionation factors. As a result, they are not capable of simulating reasonably the behavior of O isotope exchange up rock cooling. In particular, they have exaggerated the quantitative relationship between the O isotope temperature and the modal abundance of minerals in most cases. By contrast, models involving Sr diffusion among multiminerals also suggest that apparent Rb–Sr isochron ages depend on rock mode and usually differ from ages predicted by the Dodson (1973) model in certain slowly cooling closed-systems (Jenkin et al. 1995; Jenkin 1997). In a system where Sr is taken up by feldspars that behave as an infinite reservoir like the cases discussed in this study, the difference between mineral Rb–Sr ages is the closest to that estimated by Dodson's model (Jenkin 1997).

The Rb–Sr isochron constructed by the three unaltered minerals from the Yueshan quartz diorite gives the age of 137.6 ± 1.3 Ma (Table 3; Fig. 6), which agrees with the previous amphibole Ar–Ar age of 136.0 ± 1.1 Ma (Chen et al. 1991) within analytical uncertainty. Therefore, the Rb–Sr isochron age is geologically meaningful. As discussed in the previous section for the quartz monzonites east of the Tanlu fault, the meaningful Rb–Sr mineral isochron corresponds to the state of retrograde O isotope re-equilibration during cooling of the intrusions.

The age of 136.86 ± 0.85 Ma (Table 3; Fig. 5) given by the Rb–Sr isochron that is constructed by the unaltered and altered minerals from the Yueshan quartz diorite is identical to the isochron age of 137.6 ± 1.2 Ma given by the three unaltered minerals from the same intrusion. Therefore, the Rb–Sr isochron age given by the altered minerals is also geologically meaningful, although both Rb and Sr concentrations as well as both $^{87}Rb/^{86}Sr$ and $^{87}Sr/^{86}Sr$ ratios of the altered minerals all changed due to the alteration.

A simple explanation could be given based on the relative diffusivities of elements and isotopes in minerals. It is known that O diffuses faster than Sr in the same minerals under the conditions of granitoid cooling (Fig. 1). Suppose that a low-T disturbance changed the state of O isotope equilibrium, but did not affect Sr isotope system after high-T equilibrium. The Rb–Sr isochron would then remain unchanged despite the change in the state of O isotope equilibrium. However, the mineral alteration did take place but the altered minerals did not form in the Yueshan intrusion. Thus, the simple explanation based on diffusion alone is not appropriate for the Yueshan case.

Another possibility is that the alteration event is somewhat younger than the crystallization timing of the rocks, but it took place in an environment, which still had the same homogeneous $^{87}Sr/^{86}Sr$ ratio as the original magma. This scenario could be true only if Sr in the rock would mix with Sr in the assimilated material derived from an external fluid and the two components were homogenized very quickly at high temperatures. However, both Sr concentration and Sr isotopic ratios of oligoclase cannot change in several million years because of slow Sr diffusivity in the mineral (Giletti and Casserly 1994). Based on a rough estimate, $x = (Dt)^2$ where x, D and t stands for diffused distance, diffusivity and time required, it would take 25 Ma for Sr, to diffuse across over a distance of 1 mm in oligoclase even at a temperature as high as 650°C. Sr diffusion in oligoclase must be a slow process.

During the alteration of granitoids that formed at shallow and intermediate depths, fluid must be involved. Generally, an external fluid from the country rocks has elemental concentrations and isotopic compositions different from those of the igneous rock itself. Involvement of such a fluid during alteration of an igneous rock would change the elemental concentrations and isotopic ratios of igneous minerals, depending on the degree of alteration, the amount of newly formed minerals and the difference in elemental concentration and isotopic ration between the fluid and minerals. In such a case, the apparent age given by the isochron constructed by the mineral assemblage containing altered minerals may be meaningless, sometimes with large uncertainties. If a mineral of an igneous rock is highly altered by the external fluid, the isochron constructed by the mineral assemblage without the altered mineral but containing whole-rock point would also give meaningless or disturbed apparent age, because the position of the whole-rock point would deviate from the isochron due to the presence of altered minerals in the whole-rock powder.

However, the situation would be different for a rock that interacted with an internally derived (deuteric) fluid as in the case of sample Y-1 from the Yueshan body. By means of mass balance, we calculated both Rb and Sr concentrations and the Sr isotopic ratio of a ''whole-rock'' for the sample Y-1, which gives $^{87}Rb/^{86}Sr = 1.39$ and $^{87}Sr/^{86}Sr = 0.709015$. The isochron constructed by the calculated ''whole-rock,'' hornblende, unaltered and altered biotite and plagioclase yields an age of 136.85 ± 0.79 Ma, identical to that given by the isochrons without calculated whole-rock point, as predicted by the principle of mass balance. On this isochron, the whole-rock point lies somewhere between biotite and plagioclase as expected by the mass balance. The altered biotite and plagioclase are shifted towards the whole-rock point along the isochron. The data point of biotite, having both high $^{87}Rb/^{86}Sr$ and $^{87}Sr/^{86}Sr$, moves towards that of the whole-rock; whereas the data point of plagioclase, having both low $^{87}Rb/^{86}Sr$ and $^{87}Sr/^{86}Sr$, moves towards the whole-rock and biotite points that have both high $^{87}Rb/^{86}Sr$ and $^{87}Sr/^{86}Sr$. By such an internal ''adjustment,'' the element and isotopic exchange trajectories coincide with the mixing line and thus with the Rb–Sr isochron. Because the data points of the altered minerals move along the isochron, the isochron would not change by the alteration. As a result, the isochron age kept meaningful.

On the other hand, the altered biotite has a lower $\delta^{18}O$ value than the unaltered one, whereas the altered plagioclase shows a higher $\delta^{18}O$ value than that of the unaltered one (Table 1). The mass balance calculated ''whole-rock'' gives an $\delta^{18}O$ value of 7.4‰. Changes in the O isotopic ratio for different minerals from the rock can be modeled following the simple cooling model of Giletti (1986). In sample Y-1, the hornblende has the highest closure temperature of O diffusion at ~565°C (Farver and Giletti 1985) and thus ceased the O isotope exchange at first. Because $\delta^{18}O_{Hbl}$ (5.77‰) is lower than $\delta^{18}O_{wr}$, the remaining part of rock has an $\delta^{18}O_{(wr-Hbl)}$ of 7.6‰. The rock was cooled down continuously to the closure temperature for quartz (~380°C), then quartz ceased O isotope exchange with the confined fluid. Since $\delta^{18}O_Q = 10.35‰$, the closure of quartz resulted in a decrease in the O isotopic ratio for the remaining part of the rock, and the $\delta^{18}O_{(wr-Hbl-O)}$ would be about 7.3‰. By this time, only two major minerals, biotite and feldspar, could exchange their O isotopes with the confined fluid. As the temperature of the rock decreased further near to the closure temperature of biotite (about 350°C), biotite ceased the O isotope exchange. At last, feldspar is closed for O isotope exchange, but its closure temperature depends on effective diffusion radius and cooling rate.

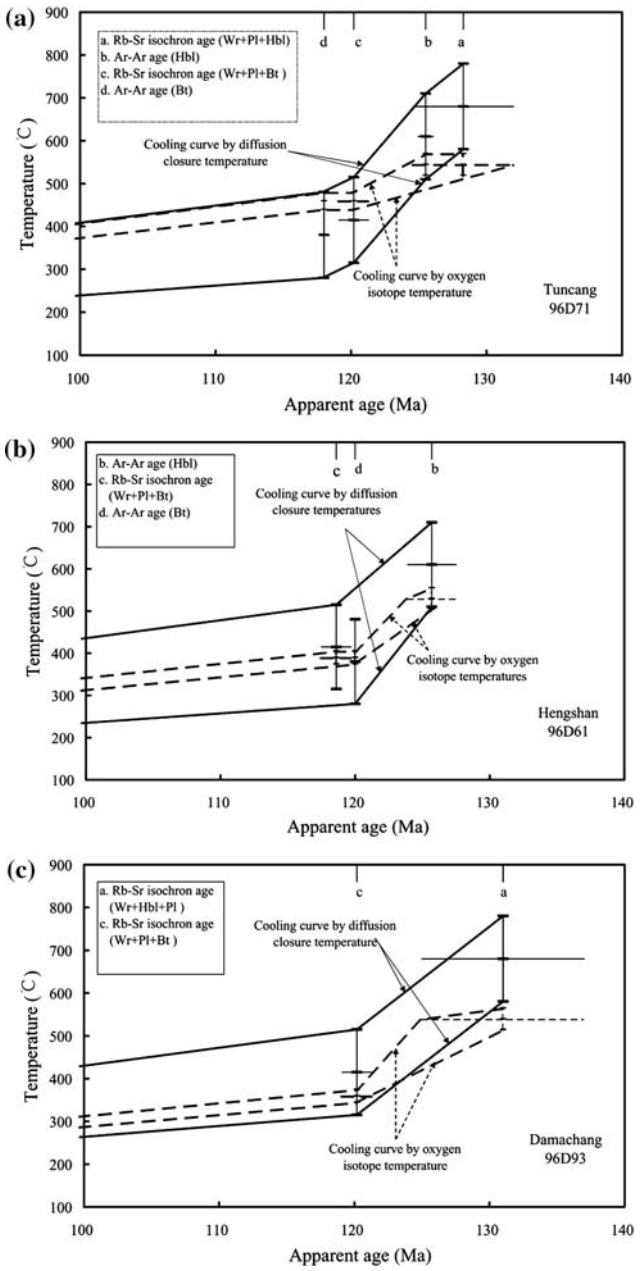

Fig. 7 Cooling curves for the quartz monzonites at **a** Tuncang, **b** Hengshan and **c** Damachang. *Solid lines* denote the cooling curves constructed by using the empirical closure temperatures of radiometric systems, and *dashed lines* using the O isotope temperatures of mineral pairs

With decreasing temperature, O isotope fractionation $\Delta^{18}O_{Pl-Bt}$ tends to increase. Based on the theoretically calibrated fractionation between quartz, biotite and plagioclase (Zheng 1993a, b) and on our observed fractionation between plagioclase and biotite from sample Y-1, an O isotopic temperature of 400 ± 30°C is obtained for the plagioclase–biotite pair. The temperature thus obtained, is close to the closure temperatures of O diffusion in quartz and biotite. Meanwhile, a lower temperature of 300 ± 20°C is calculated for the altered plagioclase and altered biotite pair by using the O isotopic fractionation between plagioclase and biotite (Zheng 1993a, b). However, the occurrence of altered minerals is evident under microscope. When the alteration took place, kaolinite formed after plagioclase and chlorite after biotite. Although O isotope fractionation between plagioclase (An = 20–30) and kaolinite is negligible, chlorite is about 1–1.5‰ higher than biotite at about 350–200°C (Zheng 1993a, b). Therefore, a low-T alteration can explain the $\delta^{18}O$ change in the minerals from the Yueshan sample.

In the case of the Yueshan quartz diorite, it is suggested that when the rock suffered an alteration by an internal fluid, O isotope fractionations between the altered minerals were changed a little bit, due to the low-T isotopic exchange. Nevertheless, the Rb–Sr isochron age remained reasonably precise and accurate because both $^{87}Rb/^{86}Sr$ and $^{87}Sr/^{86}Sr$ ratios were only slightly changed along the isochron.

Implication for construction of cooling curve for granitic intrusions

The cooling history of intrusive rocks provides important constraints on the uplift of the terrane, exhumation of deeply buried part in orogenic belts and evolution of the crust (e.g., Heizler et al. 1988; Cosca et al. 1991; Chen et al. 1995; Zheng et al. 1996; Zhao et al. 2004). Intrusive rocks with adequate geochronological and geothermometric data, such as the Tuncang, Damachang and Hengshan quartz monzonites in this study are suitable for such a practice.

There is a consensus of opinion that the apparent age given by the chronometers represents the time when the system was cooled down to the closure temperature of relevant element diffusion in the determined minerals. As a common practice, cooling curve was traditionally constructed by a combined use of Rb–Sr isochron age, Ar–Ar age and the empirical closure temperatures of element diffusion in the minerals of interest. Taking sample 96D71 from the Tuncang body as an example; the rock cooled down to 680°C (Sr closure in hornblende) at 128.3 ± 3.7 Ma (Wr + Hbl + Pl Rb–Sr isochron age) and 610°C (Ar closure in hornblende) at 125.51 ± 0.55 Ma (hornblende Ar–Ar age), to 415°C (Sr closure in biotite) at 120.2 ± 1.1 Ma (Wr + Pl + Bt Rb–Sr isochron age) and to 380°C (Ar closure in biotite) at 118.0 ± 0.1 Ma (biotite Ar–Ar age). An approximate cooling rate of about 29 ± 19°C/Ma can be estimated for the temperature interval of about 680–380°C. Then, the

rock had slowly cooled to the surface temperature at the present time (Fig. 7a).

However, the empirical estimate of the closure temperatures is associated with large uncertainties from such parameters as effective diffusion radius and modal abundance of minerals. In addition, variation in chemical composition and water content could result in a change in the diffusivity of element in the minerals of interest (e.g., Harrison et al. 1985). The exact mechanism of diffusion is difficult to define and, therefore, closure temperatures are not constant (Dodson and McClelland-Brown 1985; Giletti 1986; Eiler et al. 1993; Jenkin et al. 1994). The effective diffusion radius (not just the grain size of minerals) is not accurately known. In contrast, the determination of O isotope temperature depends on fewer assumptions. Many well-calibrated O isotope geothermometers, such as empirical estimates (e.g., Bottinga and Javoy 1975; Kohn and Valley 1998), experimental determinations (e.g., Clayton et al. 1989; Chiba et al. 1989; Matthews 1994; Chacko et al. 1996) and theoretical calculations (e.g., Zheng 1991, 1993a, b) applicable to igneous and metamorphic rocks, are available in the literature. As reviewed by Zheng (1999), most of the calibrations by the different methods are in excellent agreement with one another except the experimental calibrations of Chacko et al. (1996) for micas. Thus, they are capable of giving reasonable estimates of the apparent equilibrium temperatures of O isotope exchange by O diffusion in given minerals during cooling. In this regard, we suggest an alternative approach to construct the cooling curves by using the ages obtained from the chronometers and the corresponding O isotope temperatures for quartz and isochron mineral pairs. The geochemical basis for this practice lays in the observations that our Wr + Pl + Hbl Rb–Sr isochron ages agree with the hornblende Ar–Ar ages, the Wr + Pl + Bt Rb–Sr isochron ages agree with the biotite Ar–Ar ages in the studied samples, and that there is a general similarity in closure temperature between Sr, O and Ar in hornblende, albite and biotite, respectively. Although the different calibrations could yield somewhat different O isotope temperatures for some of mineral-pairs (Zheng 1999), it does not bring substantial differences in the temperatures when the mostly consistent calibrations are applied.

As such, sample 96D71 was cooled to about 545 ± 25°C ($T_{Q–Hbl}$) at 128.3 ± 3.7 Ma (Wr + Hbl + Pl Rb–Sr isochron age) which encompasses the hornblende Ar–Ar age of 125.51 ± 0.55 Ma, and then cooled to about 460 ± 20°C ($T_{Q–Bt}$) at 120.2 ± 1.1 Ma (Wr + Pl + Bt Rb–Sr isochron age). The estimated cooling rate is about 11 ± 6°C/Ma (Fig. 7a).

The same methodology can be applied to the other bodies from the same region. However, the Wr + Hbl + Pl Rb–Sr isochron age for the Hengshan body is not precise enough to be used for cooling curve. Sample 96D61 was cooled to 610°C (Ar closure in hornblende) at 125.7 ± 1.8 Ma (hornblende Ar–Ar age), to 415°C (Sr closure in biotite) at 118.6 ± 1.1 Ma (Wr + Pl + Bt Rb–Sr isochron age) or to 380°C (Ar closure in biotite) at 120.0 ± 0.2 Ma (biotite Ar–Ar age). An approximate cooling rate of about 25 ± 7°C/Ma can be estimated for the temperature interval of about 610–380°C (Fig. 7b). On the other hand, based on the O isotope temperatures, the sample was cooled to about 530 ± 25°C ($T_{Q–Hbl}$) at 125.7 ± 1.8 Ma (hornblende Ar–Ar age), and then to about 390 ± 15°C ($T_{Q–Bt}$) at a time interval between 118.6 ± 1.1 and 120.0 ± 0.2 Ma (Wr + Pl + Bt Rb–Sr isochron age and biotite Ar–Ar age). The estimated cooling rate is about 22 ± 2°C/Ma (Fig. 7b), consistent with that estimated based on the empirical closure temperature.

The Damachang body has only the Rb–Sr isochron ages. Based on the estimated closure temperatures, sample 96D93 was cooled to 680°C (Sr closure in hornblende) at 131 ± 6 Ma (Wr + Hbl + Pl Rb–Sr isochron age), and to 415°C (Sr closure in biotite) at 120.2 ± 1.1 Ma (Wr + Pl + Bt Rb–Sr isochron age). An approximate cooling rate of about 25 ± 18°C/Ma can be obtained (Fig. 7c). Based on the O isotope temperatures, the sample was cooled to about 540 ± 25°C ($T_{Q–Hbl}$) at 131 ± 6 Ma (Wr + Hbl + Pl Rb–Sr isochron age), and then cooled to about 360 ± 15°C ($T_{Q–Bt}$) at 120.2 ± 1.1 Ma (Wr + Pl + Bt Rb–Sr isochron age). The estimated cooling rate is about 17 ± 4°C/Ma (Fig. 7c).

The cooling curves constructed by the different methods show similar features, that is, cooled rapidly in the high temperature interval at first and then followed by a slow cooling in the low temperature range till the surface temperature at the present time. The cooling rates estimated by the two models overlap with each other for the Hengshan body (Fig. 7b), but the estimated average cooling rates based on the O isotope temperature is lower than that estimated based on the empirical closure temperature for the Tuncang and Damachang bodies (Fig. 7a, c). The difference may result either from overestimate of the Sr closure temperature in hornblende or from underestimation of the O isotope temperature for the quartz–hornblende pair.

At present, no independent evidence can be used to judge which approach is closer to the reality. The real cooling rate may lie between the two model estimates. In either case, the rocks in question are required to

behave as closed systems on the whole-rock scale for both stable and radiogenic isotope systems. They deal with different minerals, different isotope systems and possibly different mechanisms of isotope exchange. The best available way to determine the cooing rate of a granite pluton may be with a combination of U–Pb ages (zircon, monazite or titanite) and Ar–Ar ages derived from clean (unaltered) mineral separates of hornblende, biotite and K-feldspar. However, uncertainties in the closure temperatures of Pb and Ar diffusion in these minerals are still associated with uncertainties in parameters such as effective diffusion radius of minerals. In contrast, fewer variables are involved in the present estimate of cooling rates using the O isotope temperatures for the individual intrusions.

Conclusions

A combined study of mineral O and Rb–Sr isotopes for a number of Mesozoic granitoid in China demonstrates that the degree of O isotopic equilibrium between coexisting minerals is reasonably correlated with the degree of validity of mineral Rb–Sr isochrons. The state of O isotope equilibrium between isochron minerals corresponds to geologically meaningful isochron ages as long as the variation in $^{87}Rb/^{86}Sr$ ratio is large enough to provide reasonably small age uncertainties. The state of O isotope disequilibrium is often caused by interaction between the rock and the external fluid that results in mineral alteration. Therefore, the state of O isotope equilibrium between coexisting minerals provides a critical test for the validity of Rb–Sr isochron ages for the intermediate to felsic intrusions. The effect of internally or externally derived fluids on the validity of chronometric dating can also be constrained by the mineral $\delta^{18}O$ differences.

Quartz monzonites from the region east of the Tanlu fault in East-Central China yield quartz–hornblende O isotopic temperature (T_{Q-Hbl}) of 530 ± 25 to 590 ± 30°C with T_{Q-Hbl} higher than T_{Q-Bt} and T_{Q-Bt} higher than T_{Q-Pl}, suggesting retrograde re-equilibration between the minerals during cooling. Two plutons with $^{87}Rb/^{86}Sr$ ratios, larger than 1.0 give geologically meaningful Wr + Hbl + Pl Rb–Sr isochron ages of 128.3 ± 3.7 and 131 ± 6 Ma, respectively, and the same Wr + Pl + Bt isochron ages of 120.2 ± 1.1 Ma. The other two plutons give Rb–Sr ''isochron'' ages lesser than the true age and with large uncertainties, due to a small variation in Rb/Sr ratios for the minerals and alteration of feldspar.

Granites from the Yili terrane in Northwest China show a reversed sequence of O isotope temperatures ($T_{Q-Pl} > T_{Q-Bt}$) and an unreasonably high O isotope temperature of $T_{Q-Pl} > 1{,}600$°C), suggesting a state of O isotope disequilibrium between the minerals. All the three granites have large uncertainties in both ''isochron'' ages and initial isotopic ratios. Therefore, precise and geologically meaningful Rb–Sr isochron age cannot be expected if the state of O isotope equilibrium between isochron minerals is not achieved and preserved in the rock and when the range of $^{87}Rb/^{86}Sr$ is not large enough for a precise dating. In other words, if the state of O isotope disequilibrium occurs between isochron minerals, the Rb–Sr isochron age obtained will probably carry large uncertainties in both age and initial ratio and thus obscure its geological meaning.

The Yueshan quartz diorite from the Middle-Lower Yangtze region in East-Central China shows retrograde O isotope re-equilibration between the minerals during rock cooling. Unaltered minerals give a geologically meaningful Hbl + Pl + Bt Rb–Sr isochron age of 137.6 ± 1.3 Ma. However, quartz and altered mineral pairs give O isotope temperatures, marginally different from those for quartz and unaltered mineral pairs, suggesting insignificant disturbance of O isotopic systems by secondary alteration. Nevertheless, the unaltered and altered (in total six) minerals give an isochron age identical to the age given by the unaltered minerals. Despite the facts that the O isotopic system was disturbed and that both Rb and Sr concentrations as well as the Sr isotopic ratios of altered minerals were changed, the isochron age was not affected because the $^{87}Rb/^{86}Sr$ and $^{87}Sr/^{86}Sr$ ratios of altered minerals were slightly changed along the isochron. In this case, the Rb–Sr isochron could still define a geologically meaningful age when the granite was only affected by an internal fluid with the isotopic composition, identical to the whole-rock during the post-magmatic alteration.

Because most intermediate-felsic intrusions experienced rapid cooling in the early stage of their emplacement but relatively slow cooling in the late stage, an alternative approach is proposed to construct cooling curve by using the O isotope temperature of quartz–mineral pairs in coupling with the chronometric dates for the corresponding minerals. The resultant cooling rates are either similar to, or slightly different from those obtained by the traditional method, using the empirically estimated closure temperatures for radiogenic isotope diffusion in the dated minerals. The applicability of this new method merits further investigation.

Acknowledgments This study was supported by funds from the Natural Science Foundation of China (40303002, 49573172 and 49672110). We thank T.-X. Zhou, X.-C. Yang, T.-S. Gao and G. Yang for their assistance with field work, X. Zhang, X.-P. Zha and Z.-C. Peng for their assistance with laboratory analyses, G. Yu for his help with illustration. Deep appreciation also goes to Prof. W.-Z. Shen for his helpful suggestions during this study. Comments by Drs T. Chacko, S. Claesson, G.R.T. Jenkin and two anonymous reviewers are greatly helpful in improving the presentation of this manuscript.

References

Anhui (Anhui Bureau of Geology and Mineral Resourcesa) (1970) Regional geology map (in Chinese): Taihu quadrant (1:200,000). Geological Publishing House, Beijing, 26 pp

Anhui (Anhui Bureau of Geology and Mineral Resourcesb) (1987) Regional geology of Anhui Province (Geological Memoirs, ser. 1, No. 5) (in Chinese with English abstract). Geological Publishing House, Beijing, 721 pp

Bell DR, Rossman GR, Moore RO (2004) Abundance and partitioning of OG in a high-pressure magmatic system: megacrysts from the Monastery kimberlite, South Africa. J Petrol 45:1539–1564

Bottinga Y, Javoy M (1975) Oxygen isotope partitioning among minerals in igneous and metamorphic rocks. Rev Geophys Space Phys 13:401–418

Brabander DJ, Giletti BJ (1995) Strontium diffusion kinetics in amphiboles and significance to thermal history determinations. Geochim Cosmochim Acta 59:2223–2238

Brooks C, Hart SR, Wendt I (1972) Realistic use of two-error regression treatments as applied to rubidium–strontium data. Rev Geophys Space Phys 10:551–577

Chacko T, Xu X-S, Mayeda TK, Clayton RN, Goldsmith JR (1996) Oxygen isotope fractionation in muscovite, phlogopite, and rutile. Geochim Cosmochim Acta 60:2595–2608

Chen JF, Li XM, Zhou TX, Foland KA (1991) ^{40}Ar–^{39}Ar dating for the Yueshan diorite, Anhui province and the estimated formation time of the associated ore deposit. Geosicences (in Chinese with English abstract) 5(1):91–99

Chen JF, Xie Z, Liu SS, Li XM, Foland KA (1995) Cooling age of Dabie orogen, China, determined by $^{40}Ar/^{39}Ar$ and fission track techniques. Sci China B 38:749–757

Chen JF, Xie Z, Zheng Y-F, Gong B, Chen W, Zhou TX, Zhang X (2003) The relation between Rb–Sr, ^{40}Ar–^{39}Ar geochronometers and oxygen isotopic equilibrium of intrusions from eastern Anhui province, China. Geol J China Univ (in Chinese with English abstract) 9:172–184

Chiba H, Chacko T, Clayton RN, Goldsmith JR (1989) Oxygen isotope fractionations involving diopside, forsterite, magnetite, and calcite: application to geothermometry. Geochim Cosmochim Acta 53:2985–2995

Clayton RN (1981) Isotopic thermometry. In: Newton RC, et al (eds) Thermodynamics of minerals and melts. Springer, Berlin Heidelberg New York, pp. 85–109

Clayton RN, Goldsmith JR, Mayeda TK (1989) Oxygen isotope fractionation in quartz, albite, anorthite and calcite. Geochim Cosmochim Acta 53:725–733

Cong BL (ed) (1996) Ultrahigh-pressure metamorphic rocks in the Dabieshan-Sulu region of China. Kluwer Academic Publishers, Dordrecht, p 224

Cosca MA, Sutter JF, Essene EJ (1991) Cooling and inferred uplift/erosion history of the Grenville orogen, Ontario: constraints from $^{40}Ar/^{39}Ar$ thermochronology. Tectonics 10:957–977

Criss RE, Gregory RT, Taylor HP Jr (1987) Kinetic theory of oxygen isotope exchange between minerals and water. Geochim Cosmochim Acta 51:952–960

Dickin AP (1995) Radiogenic isotope geology. Cambridge University Press, Cambridge, pp. 36–47

Dodson MH (1973) Closure temperature in cooling geochronological and petrological systems. Contrib Mineral Petrol 40:259–274

Dodson MH (1979) Theory of cooling ages. In: Jaeger E, Hunziker JC (eds) Lecture in isotope geology. Springer, Berlin Heidelberg New York, pp. 194–202

Dodson MH, McClelland-Brown E (1985) Isotopic and palaeomagnetic evidence for rates of cooling, uplift and erosion. In: Snelling NJ (ed) The chronology of geological record. Geol Soc Memoir (Lond) 10:315–325

Doremus RH (2004) Transport of oxygen in silicate glasses. J Non-Cryst Solids 349:242–247

Eiler JM, Baumgartner LP, Valley JW (1992) Intercrystalline stable isotope diffusion: a fast grain boundary model. Contrib Mineral Petrol 112:543–557

Eiler JM, Valley JW, Baumgartner LP (1993) A new look at stable isotope thermometry. Geochim Cosmochim Acta 57:2571–2583

Eiler JM, Farley KA, Valley JW, Stolper EM, Hauri E, Craig H (1995) Oxygen isotope evidence against bulk recycled sediment in the source of Pitcarin island lavas. Nature 377:138–141

Ernst WG, Rumble D III (2003) Oxygen isotopic study of Late Mesozoic cooling of the Mount Barcroft area, central White Mountains, eastern California. Contrib Mineral Petrol 144:639–651

Farver JR, Giletti BJ (1985) Oxygen diffusion in amphiboles. Geochim Cosmochim Acta 49:1403–1411

Faure G (1986) Principles of isotope geology, 2nd edn. Wiley, New York, p 589

Faure G, Powell JL (1977) Strontium isotope geology. Springer, Berlin Heidelberg New York, p 188

Foland KA, Allen JC (1991) Magma sources for Mesozoic anorogenic granites of the White Mountain magma series, New England USA. Contrib Mineral Petrol 109:195–211

Fortier SM, Giletti BJ (1991) Volume self-diffusion of oxygen in biotite, muscovite, and phlogopite micas. Geochim Cosmochim Acta 55:1319–1330

Giletti BJ (1986) Diffusion effect on oxygen isotope temperatures of slowly cooled igneous and metamorphic rocks. Earth Planet Sci Lett 77:218–228

Giletti BJ (1991) Rb and Sr diffusion in alkaline feldspars, with implications for cooling histories of rocks. Geochim Cosmochim Acta 55:1331–1343

Giletti BJ, Casserly JED (1994) Strontium diffusion kinetics in plagioclase feldspars. Geochim Cosmochim Acta 58:3785–3793

Giletti BJ, Yund RA (1984) Oxygen diffusion in quartz. J Geophys Res B89:4039–4046

Giletti BJ, Semet MP, Yund RA (1978) Studies in diffusion, III. Oxygen in feldspars, an ion microprobe determination. Geochim Cosmochim Acta 42:45–57

Gladney ES, Jones EA, Nickell EJ (1990) Compilation of elemental concentration data for USGS basalt BCR1. Geostand Newsl XIV(2):209–273

Gong B, Zheng Y-F, Zhao Z-F, Chen R-X (2006) Water in granitic minerals: implications for oxygen isotope geothermometry. Geochim Cosmochim Acta 70:A213

Grant K, Gleeson SA, Roberts S (2003) The high-temperature behavior of defect hydrogen species in quartz: implications for hydrogen isotope studies. Am Mineral 88:262–270

Gregory RT, Criss RE, Taylor HP Jr (1988) Oxygen isotope exchange kinetics of mineral pairs in closed and open systems: applications to problems of hydrothermal alteration of igneous rocks and Precambrian iron formation. Chem Geol 75:1–42

Harrison TM (1981) Diffusion of ^{40}Ar in hornblende. Contrib Mineral Petrol 78:324–331

Harrison TM, Duncan I, McDougall I (1985) Diffusion of ^{40}Ar in biotite: temperature, pressure and compositional effects. Geochim Cosmochim Acta 49:2461–2468

Heizler MT, Lux DR, Decker ER (1988) The age and cooling history of the Chain of Ponds and Big Island Pond plutons and the Spider lake granite, West-central Maine and Quebec. Am J Sci 288:925–952

Hodges KV (2003) Geochronology and thermochronology in orogenic systems. Treaties Geochem 3:263–292

Huang J, Zheng Y-F, Zhao Z-F, Wu Y-B, Zhou J-B, Liu XM (2006) Melting of subducted continent: element and isotopic evidence for a genetic relationship between Neoproterozoic and Mesozoic granitoids in the Sulu orogen. Chem Geol 229:227–256

Jenkin GRT (1997) Do cooling paths derived from mica Rb–Sr data reflect true cooling paths? Geology 25:907–910

Jenkin GRT, Linklater C, Fallick AE (1991) Modeling of mineral δ^{18}O values in an igneous aureole: closed-system model predicts apparent open-system δ^{18}O values. Geology 19:1185–1188

Jenkin GRT, Farrow CM, Fallick AE, Higgins D (1994) Oxygen isotope exchange and closure temperatures in cooling rocks. J Metamorphic Geol 12:221–235

Jenkin GRT, Rogers G, Fallick AE, Farrow CM (1995) Rb–Sr closure temperatures in bi-mineralic rocks; a mode effect and test for different diffusion models. Chem Geol 122:227–240

Johnson EA, Rossman GR (2004) A survey of hydrous species and concentrations in igneous feldspars. Am Mineral 89:586–600

Juteau M, Michard AJ, Albarade F (1984) Isotopic heterogeneities in the granitic intrusion of Monte Capanne (Elba island, Italy) and dating concept. J Petrol 25:532–545

Kohn MJ, Valley JW (1998) Obtaining equilibrium oxygen isotope fractionations from rocks: theory and example. Contrib Mineral Petrol 132:209–224

Li XM, Li BX, Zhang X, Zhou TX (1985) Geochronology of Guandian rock mass in Anhui province and dynamic metamorphism in Tancheng–Lujiang fracture zone. J China Univ Sci Technol (in Chinese) 15(Suppl.):254–261

Li QL, Li SG, Zheng Y-F, Li HM, Massonne HJ, Wang QC (2003) A high precision U–Pb age of metamorphic rutile in coesite-bearing eclogite from the Dabie Mountains in central China: a new constraint on the cooling history. Chem Geol 200:255–265

Li X-P, Zheng Y-F, Wu Y-B, Chen FK, Gong B, Li Y-L (2004) Low-T eclogite in the Dabie terrane of China: petrological and isotopic constraints on fluid activity and radiometric dating. Contrib Mineral Petrol 148:443–470

Ludwig KR (1999) Isoplot—a plotting and regression program for radiogenic-isoplot data. USGS Open File Rep 91-445, pp. 1–45

Matthews A (1994) Oxygen isotope geothermometers for metamorphic rocks. J Metamorphic Geol 12:211–219

Nakashima S, Matayoshi H, Yuko T, Michibayashi K, Masuda T, Kuroki N, Yamagishi H, Ito Y, Nakamora A (1995) Infrared microspectroscopy analysis of water distribution in deformed and metamorphosed rocks. Tectonophysics 245:263–276

O'Neil JR, Chappell BW (1977) Oxygen and hydrogen isotope relations in the Berridale batholith. J Geol Soc Lond 133:559–571

Rossman GR (1996) Studies of OH in nominally anhydrous minerals. Phys Chem Minerals 23:299–304

Rumble D, Farquhar J, Young ED, Christensen CP (1997) In situ oxygen isotope analysis with an excimer laser using F_2 and BrF_5 reagents and O_2 gas as analyte. Geochim Cosmochim Acta 61:4229–4234

Sengor AMC, Natal'in BA, Burtman VS (1993) Evolution of the Altaid tectonic collage and Paleozoic crustal growth in Eurasia. Nature 364:299–307

Sharp ZD (1990) A laser-based microanalytical method for the in situ determination of oxygen isotope ratios of silicates and oxides. Geochim Cosmochim Acta 54:1353–1357

Taylor HP Jr, Sheppard SMF (1986) Igneous rocks: I. Processes of isotopic fractionation and isotope systematics. Rev Mineral 16:227-271

Tuomeur (Expedition of Tuomeur Peak, Chinese Academy of Sciences) (1985) Geology and Paleontology of Tuomeur Peak region in Tianshan (in Chinese). People's Press of Xinjiang, Urumqi, 192 pp

Valley JW (2001) Stable isotope thermometry at high temperatures. Rev Mineral Geochem 43:367–413

Valley JW, Kitchen N, Kohn MJ, Niendeorf CR, Spicuzza MJ (1995) UWG-2, a garnet standard for oxygen isotope ratio: strategies for high precision and accuracy with laser heating. Geochim Cosmochim Acta 59:5223–5231

Wendt T, Carl C (1991) The statistical distribution of the mean squared weighted deviation. Chem Geol 86:275–285

Wu R-X, Zheng Y-F, Wu Y-B, Zhao Z-F, Zhang S-B, Liu XM, Wu F-Y (2006) Reworking of juvenile crust: element and isotope evidence from Neoproterozoic granodiorite in South China. Precambrian Res 146:179–212

Xiao XC, Tang YQ, Li JY, Zhao M, Feng YM, Zhu CQ (1990) A preliminary study of the evolution of the tectonics of northern Xinjiang. Geol Xinjiang (in Chinese with English abstract) 1:47–67

Xie Z, Zheng Y-F, Jahn B-M, Ballevre M, Chen JF, Gautier P, Gao TS, Gong B, Zhou JB (2004) Sm–Nd and Rb–Sr dating for pyroxene-garnetite from North Dabie in east-central China: problem of isotope disequilibrium due to retrograde metamorphism. Chem Geol 206:137–158

Xie Z, Zheng Y-F, Zhao Z-F, Wu Y-B, Wang ZR, Chen JF, Liu XM, Wu F-Y (2006) Mineral isotope evidence for the contemporaneous process of Mesozoic granite emplacement and gneiss metamorphism in the Dabie orogen. Chem Geol 231:214–235

Xinjiang (Xinjiang Bureau of Geology and Mineral Resources) (1993) Regional geology of Xinjiang Uygur Autonomous Region (Geological Memoirs, ser. 1, No. 32) (in Chinese with English abstract). Geological Publishing House, Beijing, 841 pp

Zhang ZM, Liou JG, Coleman RG (1984) An outline of the plate tectonics of China. Geol Soc Am Bull 95:295–312

Zhang YX, Stolper EM, Wasserburg GJ (1991) Diffusion of a multi-species component and its role in oxygen and water transport in silicates. Earth Planet Sci Lett 103:228–240

Zhao Z-F, Zheng Y-F, Wei C-S, Gong B (2004) Temporal relationship between granite cooling and hydrothermal uranium mineralization at Dalongshan in China: a combined radiometric and oxygen isotopic study. Ore Geol Rev 25:221–236

Zhao Z-F, Zheng Y-F, Wei C-S, Wu Y-B, Chen FK, Jahn B-M (2005) Zircon U–Pb age, element and C–O isotope geochemistry of post-collisional mafic-ultramafic rocks from the Dabie orogen in east-central China. Lithos 83:1–28

Zheng Y-F (1989) Influences of the nature of the initial Rb–Sr system on isochron validity. Chem Geol 80:1–16

Zheng Y-F (1991) Calculation of oxygen isotope fractionation in metal oxides. Geochim Cosmochim Acta 55:2299–2307

Zheng Y-F (1993a) Calculation of oxygen isotope fractionation in anhydrous silicate minerals. Geochim Cosmochim Acta 57:1079–1091

Zheng Y-F (1993b) Calculation of oxygen isotope fractionation in hydroxyl-bearing silicates. Earth Planet Sci Lett 120:247–263

Zheng Y-F (1999) On calculations of oxygen isotope fractionation in minerals. Episodes 22:99–106

Zheng Y-F, Fu B (1998) Estimation of oxygen diffusivity from anion porosity in minerals. Geochem J 32:71–89

Zheng Y-F, Fu B, Gong B (1996) The thermal history of the Huangmeijian granite intrusion in Anhui and its relation to mineralization: isotopic evidence. Acta Geol Sin 9:168–180

Zheng Y-F, Fu B, Li Y-L, Xiao Y-L, Li S-G (1998) Oxygen and hydrogen isotope geochemistry of ultrahigh pressure eclogites from the Dabie Mountains and the Sulu terrane. Earth Planet Sci Lett 155:113–129

Zheng Y-F, Satir M, Metz P, Sharp ZD (1999a) Oxygen isotope exchange processes and disequilibrium between calcite and forsterite in an experimental C-O-H fluid. Geochim Cosmochim Acta 63:1781–1786

Zheng Y-F, Fu B, Xiao Y-L, Li Y-L, Gong B (1999b) Hydrogen and oxygen isotope evidence for fluid-rock interactions in the stages of pre- and post-UHP metamorphism in the Dabie Mountains. Lithos 46:677–693

Zheng Y-F, Wang ZR, Li SG, Zhao Z-F (2002) Oxygen isotope equilibrium between eclogite minerals and its constraints on mineral Sm–Nd chronometer. Geochim Cosmochim Acta 66:625–634

Zheng Y-F, Zhao Z-F, Li SG, Gong B (2003a) Oxygen isotope equilibrium between ultrahigh-pressure metamorphic minerals and its constraints on Sm–Nd and Rb–Sr chronometer. In: Vance D, Muller W, Villa IM (eds) Geochronology: liking the isotopic record with petrology and texture. Geol Soc Spec Publ 220:93–117

Zheng Y-F, Yang J-J, Gong B, Jahn B-M (2003b) Partial equilibrium of radiogenic and stable isotope systems in garnet peridotite during UHP metamorphism. Am Mineral 88:1633–1643

Zheng Y-F, Fu B, Gong B, Li L (2003c) Stable isotope geochemistry of ultrahigh pressure metamorphic rocks from the Dabie-Sulu orogen in China: implications for geodynamics and fluid regime. Earth Sci Rev 62:105–161

Zheng Y-F, Satir M, Metz P (2004a) Oxygen isotope exchange and disequilibrium between calcite and tremolite in the absence and presence of an experimental C-O-H fluid. Contrib Mineral Petrol 146:683–695

Zheng Y-F, Wu Y-B, Chen FK, Gong B, Li L, Zhao Z-F (2004b) Zircon U–Pb and oxygen isotope evidence for a large-scale ^{18}O depletion event in igneous rocks during the Neoproterozoic. Geochim Cosmochim Acta 68:4145–4165

Zheng Y-F, Zhou J-B, Wu Y-B, Xie Z (2005) Low-grade metamorphic rocks in the Dabie-Sulu orogenic belt: a passive-margin accretionary wedge deformed during continent subduction. Int Geol Rev 47:851–871